Towards Accurate Phase Equilibrium Modeling for Hydrogen Sulfide/Water Mixtures

By

Shiyu Yin

A Thesis Submitted in Partial Fulfillment of the Requirements for the Degree of

Master of Science

in

Petroleum Engineering

Department of Civil and Environmental Engineering

University of Alberta

ABSTRACT

Many deep gas wells contain acid gas components. Hydrogen sulfide (H_2S) is one of the typical acid gases. Accurate flow simulations for H_2S/H_2O mixtures in reservoirs and wellbores require a proper thermodynamic model that is capable of accurately modeling the H_2S/H_2O mixtures under in-situ conditions. This study aims at screening and developing cubic-equation-of-state-based thermodynamic models that can well describe the phase behaviour of H_2S/H_2O mixtures. Peng-Robinson equation of state (PR EOS) (Peng and Robinson, 1976) and Huron-Vidal (HV) (Huron and Vidal, 1979) mixing rule are used as the basic modeling framework. The temperature-dependent binary interaction parameter (BIP) correlations in the HV mixing rule are established by matching the measured vapor-liquid/liquid-liquid equilibria (VLE/LLE) data for H_2S/H_2O mixtures collected from the literature. The experimental VLE/LLE data cover a temperature range of 273.150-627.85 K and a pressure range of 0.4-302.7 bar, while the experimental density data cover a temperature range of 294.35-705.53 K and pressures up to 350 bar. Different volume translation strategies are examined in terms of their accuracy in reproducing the measured density data for H_2S/H_2O mixtures. We employ PR EOS together with the optimal BIP strategy in the HV mixing rule to reproduce the mutual solubility of H_2S and H_2O in VLE/LLE. The calculated results show a good agreement with the experimental data, especially at high temperatures and pressures; the average absolute percentage deviation (*%AAD*) of 4.90% and 4.95% can be obtained for reproducing the vapor-phase H_2O solubility and the aqueous-phase H_2S solubility, respectively. With the inclusion of the volume translation model proposed by Abudour *et al.* (2013), PR EOS together with the optimal BIP strategy in the HV mixing rule shows a good performance in estimating the aqueous-phase density for H_2S/H_2O mixtures, i.e., an %*AAD* of 5.42% in reproducing the measured density data.

DEDICATION

This dissertation is dedicated to my dearest parents, Mr. Donghai Yin and Mrs. Lihua Shen.

ACKNOWLEDGMENTS

I would like to express my sincere gratitude to my supervisor, Dr. Huazhou Li. He taught me not only how to conduct research but also a lot of professional skills useful for my future career. In addition, I want to thank my examination committee chair, Dr. Nobuo Maeda, and the examination committee members, Dr. Juliana Leung and Dr. William Zhang for their critical and valuable comments. I am grateful for the financial and spiritual support from my family, friends and colleagues in Dr. Li's research group. Finally, I also greatly acknowledge an Early Career Research Award provided by Faculty of Engineering at the University of Alberta to H. Li.

TABLE OF CONTENTS

LIST OF TABLES

LIST OF FIGURES

CHAPTER 1 INTRODUCTION

1.1 Research Background

Hydrogen sulfide (H_2S) gas is one of the most common acid gases in natural gas reservoirs. H_2S is not only toxic to human[1-2] but also corrosive to the drilling and production facilities[3-4]. H_2S can be highly dissolvable in H_2O. In order to accurately simulate the flow of water/natural-gas mixtures (containing H_2S) in reservoirs and wellbores, an accurate thermodynamic model (such as one based on Peng-Robinson equation of state (PR EOS[5])) for describing the vapor-liquid/liquid-liquid equilibria (VLE/LLE) of water/natural-gas mixtures is required[6-9]. As part of the overall modeling framework, an appropriate mixing rule together with its binary interaction parameters (BIP) should be capable of well capturing the VLE/LLE of H_2S/H_2O mixtures.

1.2 Literature Review of Existing VLE/LLE and Volume Translation Models

1.2.1 Thermodynamic Models for Predicting VLE/LLE of Gas/Water Binaries

Cubic equation of states (CEOS) such as PR EOS[5] and SRK EOS[10] have been widely used to predict the phase equilibria and density of petroleum fluids in reservoir simulations[11-15,17,19-21]. However, the conventional CEOS have certain deficiencies in modeling the phase equilibria and density of the systems that contain H_2S. A few efforts have been made to improve the correlative and predictive abilities of thermodynamic models in capturing the phase equilibria of gas/water mixtures by modifying CEOS and BIP in various mixing rules[11, 13-15, 18-19]. Carroll and Mather[11] attempted to model the phase equilibria of H_2S/H_2O mixtures by using Peng-Robinson-Stryjek-Vera (PRSV) EOS with the Stryjek-Vera (SV) mixing rule. However, Their model[11] does not perform well in reproducing the experimental data at low pressures (P<10 bar) and high temperatures (T>450 K). In 1992, Søreide and Whitson[13] proposed models to predict the mutual

solubility of CO_2/H_2O, CH_4/H_2O and H_2S/H_2O binaries by using a modified PR EOS[5]. The original van der Waals (vdW) one-fluid mixing rule was modified in their work by assigning two different BIP sets for vapor and aqueous phases. Unfortunately, Søreide and Whitson's[13] model shows a lower accuracy for H_2S/H_2O binaries than that for CO_2/H_2O and CH_4/H_2O binaries. Also, a recent study shows that the use of two different BIP sets for vapor and aqueous phases may lead to convergence issues in the multiphase equilibrium calculations[14]. Modification in BIP has also been attempted by Abudour *et al.*[15] to improve the prediction of mutual solubility for coalbed gas/water systems (such as CO_2/H_2O, CH_4/H_2O and N_2/H_2O mixtures). They developed BIP correlations as a function (both linear and quadratic) of temperatures, together with PR EOS, for modeling the phase behavior of coalbed gas/water mixtures. Abudour *et al*.[15] reported that their model is capable of reasonably well describing the phase equilibria of coalbed gases/water systems over a wide range of temperature/pressure conditions. Nevertheless, the model proposed by Abudour *et al.*[15] has not been proved to be valid for the H_2S/H_2O systems. Duan *et al.*[16] developed a 15-parameter-EOS semi-empirical model for H_2S/H_2O binaries. However, Zhao *et al.*[17] pointed out that the vapor phase prediction is compromised in Duan *et al*. model[16], and it is not recommended for vapor phase calculations. A similar issue also exists in the work by Akinfive *et al.*[18] Recently, Zhao *et al.*[17] proposed a model based on PRSV EOS, non-randomness-two-liquid (NRTL) model and Wong-Sandler (WS) mixing rule[19]. This model provides good predictions for computing the mutual solubility of H_2S and H_2O over a wide range of temperatures and pressures. However, Zhao *et al.* model[17] adopts 4 individual BIP values for each isotherm rather than generalized temperature-dependent BIP correlations. As such, linear interpolation is needed to find out the BIP values at other temperatures. Zhao *et al.*[17] also attempted to reproduce measured volumes for one H_2S/H_2O mixture, but the calculated results

from their model showed relatively large deviations from the measured volume data. A comprehensive review of the available models for describing the VLE/LLE of H_2S/H_2O binaries can be found in Zhao *et al.*[17].

1.2.2 Volume Translation Models

The aqueous-phase density prediction for H_2S/H_2O mixtures is usually inaccurate when using conventional CEOS[20,21]. In order to overcome this limitation, volume translation (VT) was introduced. The form of volume translation ranges from being a constant correction term to a more complex temperature-dependent function. Generally, the constant correction term (as proposed by Peneloux *et al.*[22] for SRK EOS[10]) is not accurate enough at high temperatures. Some researchers have also proposed temperature-dependent volume translation methods. In 1989, Chou and Prausnitz[23] provided a phenomenological correction to SRK EOS[10] by proposing a distance-function-based volume translation function. The distance function in their work depends on temperature and pressure, and accounts for the difference between predicted and actual densities. Magoulas and Tassios[24] developed a temperature-dependent volume translation correction to PR EOS for n-alkanes (C_1-C_{20}). Tsai and Chen[25] introduced a three-parameter temperature-dependent volume translation function for PR EOS to calculate vapor pressure and molar volume for more than 100 compounds. Lin and Duan[26] proposed a temperature-dependent volume translation for PR EOS to improve liquid density prediction for non-polar and slightly polar fluids. Although most of the temperature-dependent volume translation models improve the predictions of saturated liquid density, they do not perform equally well in reproducing density of liquid phase or supercritical states[26]. Later, Blaed *et al.*[27] proposed a temperature-dependent volume translation dedicated to single-phase density prediction at high temperature/pressure conditions. In 2013, Abudour *et al.*[28] proposed a volume translation method for PR EOS[8] that is

capable of accurately predicting binary-mixture density over a large temperature/pressure range. Abudour *et al.*[28] showed that their method has less complexity, maintains thermodynamic consistency (no pressure-volume isotherm crossovers in single-phase region at high pressures), and can be applied to mixtures containing highly-polar and hydrogen-bonded fluids. Recently, Shi *et al.*[21] proposed an exponential-type volume translation model that is only temperature dependent and only gives isotherm crossover issue at high temperature/pressure conditions. Furthermore, Young *et al.*[29] also demonstrated the superior advantages of applying Abudour *et al.*[28] volume translation model[27] in density calculations. They showed that, among eight evaluated volume translation models, the one proposed by Abudour *et al.*[28] presented the best results in predicting saturated liquid densities without presenting any inconsistency along the entire analyzed range.

1.3 Problem Statement

The above discussion indicates that the existing thermodynamic models have certain drawbacks in predicting the VLE/LLE of this binary system. The conventional CEOS with vdW rule is not capable of providing accurate phase equilibrium modeling for H_2S/H_2O mixtures. The aqueous-phase density estimation for H_2S/H_2O mixtures by the original PR EOS[5] is not satisfactory. Although Zhao *et al*. model[17] provides good accuracy in reproducing the VLE/LLE of H_2S/H_2O mixtures, it is inconvenient to use and cannot provide accurate aqueous-phase density predictions. Therefore, a thermodynamic model that is capable of accurately modeling the VLE/LLE and predicting aqueous-phase density of H_2S/H_2O mixtures needs to be developed.

1.4 Objectives

The main objective of this research is to achieve improved VLE/LLE and density modeling for H_2S/H_2O mixtures. The detailed objectives are:

- To conduct a critical review of the existing thermodynamic models dedicated to describing the phase equilibria of H_2S/H_2O binary systems and investigate their pros and cons;
- To design appropriate BIP strategies in Huron-Vidal (HV) mixing rule[30] that should be correlative and easy to apply under different pressure/temperature conditions;
- To select the best BIP strategy, accordingly develop temperature-dependent BIP correlations in Huron-Vidal mixing rule[30] and couple them with PR EOS[5] to well capture the VLE/LLE of H_2S/H_2O mixtures; and
- To employ the state-of-art volume translation model (i.e., Abudour *et al.* model[28]) to well reproduce the measured phase densities of H_2S/H_2O mixtures.

1.5 Thesis Structure

This thesis is organized as flows:

- **Chapter 1** introduces research background, literature review, problem statement, research objectives, and thesis structure.
- **Chapter 2** presents the methodology employed in this thesis, including all the fundamental equations and models, data collection and screening method, objective functions and error indices, BIP strategies and two-phase flash calculations.
- **Chapter 3** demonstrates the performance of the optimal BIP strategy in reproducing VLE/LLE data, and the performance of volume translated-PR EOS in predicting density data. Comprehensive comparisons of measured VLE/LLE and density of H_2S/H_2O mixtures against calculated ones from different models are also presented in this chapter.
- **Chapter 4** summarizes the conclusions achieved in this study as well as the recommendations for future work.

References

[1] Reiffenstein, R. J.; William, C.H.; Sheldon, H. R. Toxicology of Hydrogen Sulfide. *Annu. Rev*. *Pharmacol.* **1992**, *32*, 109-134.

[2] Beauchamp, R. O.; James, S. B.; James, A. P.; Craig A. J. B.; Dragana, A. A.; Philip, L. A. Critical Review of the Literature on Hydrogen Sulfide Toxicity. *Crit. Rev. Toxicol.* **1984**, *13*, 25-97.

[3] Ning, J.; Zheng, Y.; Young, D.; Brown, B.; Nešić, S. Thermodynamic Study of Hydrogen Sulfide Corrosion of Mild Steel. *Corrosion* **2013**, *70*, 375-389.

[4] Ewing, S. P. Electrochemical Studies of the Hydrogen Sulfide Corrosion Mechanism. *Corrosion* **1955**, *11*, 51-55.

[5] Peng, D. Y.; Robinson, D. B. A New Two-Constant Equation of State. *Ind. Eng. Chem. Fundam.* **1976**, *15*, 59–64.

[6] Zhang, J.; Wang, Z.; Liu, S.; Zhang, W.; Yu, J.; Sun, B. Prediction of Hydrate Deposition in Pipelines to Improve Gas Transportation Efficiency and Safety. *Appl. Energy* **2019**, *253,* 113521.

[7] Wang, Z.; Zhang, J.; Sun, B.; Chen, L.; Zhao, Y.; Fu, W. A New Hydrate Deposition Prediction Model for Gas-Dominated Systems with Free Water. *Chem. Eng. Sci.* **2017**, *163*, 145-154.

[8] Fu, W.; Wang, Z.; Zhang, J.; Cao, Y.; Sun, B. Investigation of Rheological Properties of Methane Hydrate Slurry with Carboxmethylcellulose. *J. Petrol. Sci. Eng.* **2020**, *184*, 106504.

[9] Duan, Z.; Hu, J.; Li, D.; Mao, S. Densities of the CO_2–H_2O and CO_2–H_2O–NaCl Systems up to 647 K and 100 MPa. *Energy Fuels* **2018**, *22*, 1666-1674.

[10] Soave, G. Equilibrium Constants from a Modified Redlich-Kwong Equation of State. *Chem. Eng. Sci.* **1972**, *27*, 1197-1203.

[11] Carroll, J. J.; Mather, A. E. Phase Equilibrium in the System Water-Hydrogen Sulphide: Modelling the Phase Behavior with an Equation of State. *Can. J. Chem. Eng.* **1989**, *57*, 999-1003.

[12] Chapoy, A.; Mohammadi, A. H.; Tohidi, B.; Valtz, A.; Richon, D. Experimental Measurement and Phase Behavior Modeling of Hydrogen Sulfide−Water Binary System. *Ind. Eng. Chem. Res.* **2005**, *44*, 7567-7574.

[13] Søreide, I.; Whitson, C. H. Peng-Robinson Predictions for Hydrocarbons, CO_2, N_2, and H_2S with Pure Water and NaCl Brine. *Fluid Phase Equilib.* **1992**, *77*, 217-240.

[14] Li, R.; Li, H. Improved Three-Phase Equilibrium Calculation Algorithm for Water/Hydrocarbon Mixtures. *Fuel* **2019**, *15*, 517-527.

[15] Abudour, A. M.; Sayee, A. M.; Khaled, A. M. G. Modeling High-Pressure Phase Equilibria of Coalbed Gases/Water Mixtures with the Peng–Robinson Equation of State. *Fluid Phase Equilib.* **2012**, *319*, 77-89.

[16] Duan, Z.; Sun, R.; Liu, R.; Zhu, C. Accurate Thermodynamic Model for the Calculation of H_2S Solubility in Pure Water and Brines. *Energy Fuels* **2007**, *21*, 2056-2065.

[17] Zhao, H.; Fang, Z.; Jing, H.; Liu, J. Modeling Vapor-Liquid Phase Equilibria of Hydrogen Sulfide and Water System Using a Cubic EOS-G^{EX} Model. *Fluid Phase Equilib.* **2019**, *484*, 60-73.

[18] Akinfiev, N. N.; Majer, V.; Shvarov, Y. V. Thermodynamic Description of H_2S–H_2O–NaCl Solutions at Temperatures to 573 K and Pressures to 40 MPa. *Chem. Geol.* **2016**, *424*, 1-11.

[19] Wong, D. S. H.; Sandler, S. I. A. Theoretically Correct Mixing Rule for Cubic Equation of State. *AIChE J*. **1992**, *5*, 671-680.

[20] Abudour, A. M.; Mohammad, S. A.; Robinson Jr, R. L.; Khaled, A. M. G. Volume-Translated Peng-Robinson Equation of State for Saturated and Single-Phase Liquid Densities. *Fluid Phase Equilib.* **2012**, *335*, 74-87.

[21] Shi, J.; Li, H.; Pang, W. An Improved Translation Strategy for PR EOS without Crossover Issue. *Fluid Phase Equilib*. **2018**, *470*, 164-175.

[22] Peneloux, A.; Rauzy, E.; Freze, R. A Consistent Correction for Redlich-Kwong-Soave Volume. *Fluid Phase Equilib*. **1982**, *8*, 7-23.

[23] Chou, G. F.; Prausnitz, J. M. A Phenomenological Correction to an Equation of State for the Critical Region. *AIChE J*. **1989**, *35*, 1487-1496.

[24] Magoulas, K.; Tassios, D. Thermophysical Properties of Normal-Alkanes from C_1 to C_{20} and Their Prediction for Higher Ones. *Fluid Phase Equilib*. **1990**, *56*, 119-140.

[25] Tsai, J. C.; Chen, Y. P. Application of a Volume-Translated Peng-Robinson Equation of State on Vapor-Liquid Equilibrium Calculations. *Fluid Phase Equilib*. **1998**, *145*, 193-215.

[26] Lin, H.; Duan, Y. Y. Empirical Correction to the Peng-Robinson Equation of State for the Saturated Region. *Fluid Phase Equilib*. **2005**, *233*, 194-203.

[27] Baled, H.; Enick, R. M.; Wu, Y.; McHugh, M. A.; Burgess, W.; Tapriyal, D.; Morreale, B. D. Prediction of Hydrocarbon Densities at Extreme Conditions Using Volume-Translated SRK and PR Equation of State Fit to High Temperature, High Pressure PVT Data. *Fluid Phase Equilib*. **2012**, *317*, 65-76.

[28] Abudour, A. M.; Mohammad, S. A.; Robinson Jr, R. L.; Khaled, A. M. G. Volume-Translated Peng-Robinson Equation of State for Liquid Densities of Diverse Binary Mixtures. *Fluid Phase Equilibr*. **2013**, *349*, 37-55.

[29] Young, A. F.; Pessoa, F. L. P.; Ahón, V .R. R. Comparison of Volume Translation and Co-Volume Functions Applied in the Peng-Robinson EOS for Volumetric Corrections. *Fluid Phase Equilib*. **2017**, *435*, 73-87.

[30] Huron, M. J.; Vidal, J. New Mixing Rules in Simple Equations of State for Representing Vapour-Liquid Equilibria of Strongly Non-Ideal Mixtures. *Fluid Phase Equilib*. **1979**, *3*, 255-271.

CHAPTER 2 METHODOLOGY

2.1 PR EOS Model

The PR EOS[1] is given as:

$$P = \frac{RT}{v-b} - \frac{a(T)}{v(v+b)+b(v-b)} \tag{1}$$

where

$$a(T) = \frac{0.45724\alpha(T)R^2T_c^2}{P_c^2} \tag{2}$$

$$b = \frac{0.07780RT_c}{P_c} \tag{3}$$

where P is pressure, R is the universal gas constant, T is temperature, v is molar volume, a and b are the attraction and repulsion parameters, respectively, T_c and P_c are critical temperature and critical pressure, respectively.

In equation (2), we use the alpha function proposed by Twu *et al.*[2] since it allows accurate and consistent vapor pressure prediction for substances with high polarity (e.g., water) and low boiling points (e.g., H_2S)[3]. Besides, coupled with CEOS and a proper mixing rule, it is capable of well describing the phase equilibria of polar/non-polar mixtures. The alpha function developed by Twu *et al.*[2] is given as:

$$\alpha(T_r) = T_r^{N(M-1)} exp\left[L\left(1-T_r^{MN}\right)\right] \tag{4}$$

where T_r is the reduced temperature, L, M and N are three coefficients. According to Martinez *et al.*[4], the parameters in equation (4) are L=0.1122, M=0.8688 and N=2.2734 for pure H_2S, and L=0.3872, M=0.8720 and N=1.9668 for H_2O.

2.2 HV Mixing Rule and Its BIPs

The choice of mixing rules and mixing rule parameters is important for modeling phase equilibria of gas and water systems. HV mixing rule[5] combines EOS model with an excess Gibbs energy model to improve the accuracy of phase equilibrium calculation for the systems containing polar components (e.g., water). Lindeloff and Michelsen[3] pointed out that the HV mixing rule[5] is capable of handling strongly non-ideal mixtures at high pressures, such as water-inclusive mixtures. If no polar compounds are present in the mixture, the HV mixing rule[5] can be reduced to the classical quadratic mixing rule[6]. Hence, the versatile HV mixing rule[5] is selected to be used in this study:

$$a_m = b_m \left[\sum_{i=1}^{n} z_i \frac{a_i}{b_i} - \frac{G_\infty^E}{C^*} \right] \tag{5}$$

$$b_m = \sum_{i=1}^{n} \sum_{j=1}^{n} z_i z_j \frac{\left(b_i + b_j\right)}{2} \tag{6}$$

where z_i is the mole fraction of the ith component, and C^* is 0.62323 for PR-EOS, n is number of components and G_∞^E is the excess Gibbs energy at infinite pressure that can be calculated as below[5]:

$$G_\infty^E = \sum_{i=1}^{n} z_i \frac{\sum_{j=1}^{n} G_{ji} C_{ji} z_j}{\sum_{k=1}^{n} G_{ki} z_k} \tag{7}$$

where

$$G_{ij} = b_i \exp\left(c \frac{C_{ij}}{RT} \right) \qquad G_{ij}=0 \text{ when } i=j \tag{8}$$

$$C_{ji} = g_{ji} - g_{ii} \tag{9}$$

$$g_{ii} = -C^* \frac{a_i}{b_i} \tag{10}$$

$$g_{ij} = -2\frac{\sqrt{b_i b_j}}{b_i + b_j}\sqrt{g_{ii} g_{jj}}(1 - k_{ij}) \tag{11}$$

where the term "c" in equation (8) is the adjustable mixing-rule constant and the term "k_{ij}" in equation (11) is the adjustable BIP parameter. For simplicity, we define c and k_{ij} as BIPs in this work. k_{ij} can normally take a value between -1 and 1 for different binary mixtures.

If the HV mixing rule[5] is used, the fugacity coefficient should be modified to,

$$\ln \varphi_i = \frac{b_i}{b_m}(Z-1) - \ln(Z-B) - \frac{1}{2\sqrt{2}}\left(\frac{a_i}{b_i RT} + \frac{\ln \gamma_i}{A}\right)\ln\left(\frac{Z + (1+\sqrt{2})B}{Z + (1-\sqrt{2})B}\right), i = 1, ..., n \tag{12}$$

where a_i and b_i can be calculated from equations 2-3, respectively. n is the number of components. Z is the compressibility factor calculated from PR EOS[1]. The terms A and B can be calculated as below:

$$A = \frac{a_m p}{R^2 T^2} \tag{13}$$

$$B = \frac{b_m p}{RT} \tag{14}$$

where a_m and b_m can be calculated from equations 5-6, respectively.

$\ln\gamma_i$ is the activity coefficient of each component which can be calculated as below[7],

$$\ln \gamma_i = \frac{\sum_{j=1}^{n} \frac{C_{ji}}{RT} z_j b_j G_{ji}}{\sum_{k=1}^{n} z_k G_{ki}} + \sum_{j=1}^{n} \left[\frac{z_j G_{ij}}{\sum_{k=1}^{n} z_k G_{kj}} \left(\frac{C_{ij}}{RT} - \frac{\sum_{l=1}^{n} z_l \frac{C_{li}}{RT} G_{lj}}{\sum_{k=1}^{n} z_k G_{kj}} \right) \right], i = 1,...n \quad (15)$$

2.3 Volume Translation Model

In this work, two different volume translation models (constant and Abudour *et al.* volume translation model[8]) are applied to calculate the aqueous density of H_2S/H_2O mixtures; no vapor phase density data are reported in the literature. According to Peneoux *et al.*[6], the constant volume translation model can be expressed as:

$$v = v^{EOS} - \sum_{i=1}^{n} z_i c_i \quad (16)$$

where v is the corrected molar volume, v^{EOS} is the molar volume calculated by the untranslated PR EOS, n is the number of components, and c_i is the volume-shift correction parameter of the ith component. The optimal volume shifts for H_2S and H_2O are found to be c_{H2S} = -2.5075 and c_{H2O} = 5.2711 by Martinez *et al.*[4]

Abudour *et al.* volume translation model[8] is capable of providing accurate density estimation for binary mixtures containing water. The volume translation model proposed by Abudour *et al.*[8] for a given mixture is given as:

$$v_{VTPR} = v_{PR} + c_m - \delta_{cm} \left(\frac{0.35}{0.35 + d_m} \right) \quad (17)$$

where v_{VTPR} and v_{PR} are the translated molar volumes and untranslated molar volumes, and c_m is given as[8]:

$$c_m = \left(\frac{RT_{cm}}{P_{cm}}\right)\left[c_{1m} - \left(0.004 + c_{1m}\right)\exp\left(-2d_m\right)\right] \tag{18}$$

where

$$c_{1m} = \sum_{i=1}^{n} x_i \left(0.4266 Z_{ci} - 0.1101\right) \tag{19}$$

where T_{cm} and P_{cm} are critical temperature and critical pressure of the mixture, d_m is the dimensionless distance function, and Z_{ci} is critical compressibility factor of the ith component. Based on Chou and Pransnitz[9], the dimensionless distance d_m can be described by:

$$d_m = \frac{1}{RT_c}\left(\frac{\partial P^{EOS}}{\partial \rho}\right)_T = \frac{v_{PR}^2}{RT_{cm}}\left[\frac{RT}{\left(v_{PR} - b\right)^2} - \frac{2a\left(v_{PR} + b\right)}{\left(v_{PR}^2 + 2bv_{PR} - b^2\right)^2}\right] \tag{20}$$

In equation (17), the term δ_{cm} is the volume correction for a mixture at the critical point and can be written as[8]:

$$\delta_{cm} = v_{cm}^{PR} - v_{cm} \tag{21}$$

where v_{cm}^{PR} is the critical molar volume of the mixture as calculated by PR EOS and v_{cm} is the true critical molar volume of the mixture. v_{cm}^{PR} and v_{cm} are given as[8]:

$$v_{cm}^{PR} = 0.3074\left(\frac{RT_{cm}}{P_{cm}}\right) \tag{22}$$

$$v_{cm} = \sum_{i=1}^{n} \theta_i v_{ci} \tag{23}$$

where v_{ci} is the critical molar volume of the ith component and θ_i is the surface fraction of the ith component that can be calculated by[8-9]:

$$\theta_i = \frac{x_i v_{ci}^{2/3}}{\sum_{i=1}^{n} x_i v_{ci}^{2/3}} \tag{24}$$

where x_i is the mole fraction of the ith component.

Finally, the critical temperature (T_{cm}), critical pressure (P_{cm}) and acentric factor (ω_m) of the mixture can be estimated by equations 25, 26 and 27, respectively[8]:

$$T_{cm} = \sum_{i=1}^{n} \theta_i T_{ci} \tag{25}$$

$$P_{cm} = \frac{\left(0.2905 - 0.085\omega_m\right) RT_{cm}}{v_{cm}} \tag{26}$$

$$\omega_m = \sum_{i=1}^{n} x_i \omega_i \tag{27}$$

where T_{ci} is the critical temperature of the ith component and ω_i is the acentric factor of the ith component.

2.4 Data Collection and Screening

Table 1 summarizes the experimental phase behavior data of H_2S/H_2O mixtures reported by 14 peer-reviewed articles[10-23]. The collected data cover a temperature range of 273.150-627.85 K and a pressure range of 0.4-302.7 bar. In this work, the data shown in **Table 1** are used for selecting the optimum BIP strategy (c and k_{ij}) in the HV mixing rule. **Table 2** lists the experimental density data for H_2S/H_2O mixtures reported in the literature[24-26]. It is noted from

Table 2 that only aqueous-phase density data are reported in the literature. Moreover, according to Zhao *et al.*[27], at temperatures above 530 K and pressures below 1000 bar, the phase envelope of H_2S/H_2O mixtures shrinks as temperature increases. Zhao *et al.*[27] also presented that at around 627 K, the two-phase region of H_2S/H_2O binary systems almost disappears. Therefore, for density calculations, we only employ the data below 600 K to ensure that the H_2S/H_2O mixtures remain in the two-phase region.

Table 1. Experimental phase behavior data of H_2S/H_2O mixtures reported in the literature[10-23]

T **(K)**	***P*** **(bar)**	x_{H2S} **(mol%)**[a]	y_{H2S} **(mol%)**[b]	**No. of data points**	**Footnotes**	**References**
278.15-333.15	0.4-4.9	0.066-0.699	75.517-99.546	102	-	[10]
310.93-444.26	7-87	0.29-4.63	39.81-99.60	68	c	[11]
303.15-443.15	17-23	0.463-3.077	52.76-99.850	78	-	[12]
273.150-323.135	0.46777-0.96298	0.04801-0.30497	77.499-99.240	72	-	[13]
283.15-453.15	2.23-66.70	0.080-3.998	-	206	-	[14]
363.15-423.15	14.81-33.64	-	73.500-93.600	15	-	[14]
304.05-627.85	7.01-192.49	0.749-1.402	-	121	d	[15]
344.30-477.60	29.27-208.02	0.562-9.690	-	20	-	[16]
398.15-367.65	1.01	0.016-0.420	-	39	-	[17]
313.15 -378.15	28.0-92.4	0.023-0.376	-	5	-	[18]
293.95-594.15	2.22-138.61	0.0102-1.5546	7.7700-99.6061	96	-	[19]
313.15-313.18	47.04-248.95	0.5981-3.0044	-	9	-	[20]
298.16-338.34	4.83-39.62	0.435-3.507	-	31	-	[21]
298.16-318.21	5.03-27.78	-	78.72-98.80	15		[21]
323.1-393.1	17.2-302.7	1.75-6.03	-	12	-	[22]
393.15-423.15	17-203	0.912-6.360	-	6	-	[23]

a: Solubility of H_2S in aqueous phase.

b: Solubility of H_2S in H_2S-rich phase.
c: Duan *et al.*[28] and Zhao *et al.*[27] mentioned that the measured solubility of H_2S at high pressures (P>100 bar) from Selleck *et al.*[11] shows an opposite trend to others. Carroll and Mather[18] also concluded that the data from Selleck *et al.*[11] above 100 bar are not reliable. Therefore, the data reported by Selleck *et al.*[11] at pressures above 100 bar are not included for error analysis in later sections.
d: Duan *et al.*[28] pointed out that some of Drummond's [15] data (between 310 K and 350 K) deviate from the general data set by more than 10%.

Table 2. Experimental density data of H_2S/H_2O mixtures reported in the literature[24-26]

***T* (K)**	***P* (bar)**	**Data Type[a]**	**No. of Data points**	**References**
310.95-444.25	18.8-130.0	Aqueous phase	10	[24]
294.35-314.15	1.01-18.24	Aqueous phase	26	[25]
298.15-705.53	10-350	Aqueous phase	30	[26]

a: Data type indicates the type of the collected measured data; Aqueous phase represents that only aqueous phase density data are reported.

2.5 Objective Functions and Error Indices

All the collected experimental data can be divided into three categories: (1) *T-P-x* (most of the data); (2) *T-P-y* (only few measurements are available); and (3) *T-P-x-y* (only few measurements are available). All these data are used for regressing BIPs (i.e., c and k_{ij}) in the HV mixing rule. In our study, the BIP regression only depends on temperature, such that c and k_{ij} can only be either temperature-depended or constant. The optimal values of c and k_{ij} at each isotherm are determined by minimizing properly defined objective functions. The form of the objective functions used depends on the category of the available data (e.g., *T-P-x*, *T-P-y* or *T-P-x-y*).

If the *T-P-x* data are available for BIP determination, the following objective function is used:

$$F = \sum_{i=1}^{NDP} \sum_{j=1}^{n} \left| \frac{x_{j,i}^{\exp} - x_{j,i}^{cal}}{x_{j,i}^{\exp}} \right| \tag{28}$$

If the *T-P-y* data are available, the following objective function is used:

$$F = \sum_{i=1}^{NDP} \sum_{j=1}^{n} \left| \frac{y_{j,i}^{\exp} - y_{j,i}^{cal}}{y_{j,i}^{\exp}} \right| \tag{29}$$

If the *T-P-x-y* data are available, the following objective function is used:

$$F = \sum_{i=1}^{NDP} \sum_{j=1}^{n} \left[\left| \frac{x_{j,i}^{\exp} - x_{j,i}^{cal}}{x_{j,i}^{\exp}} \right| + \left| \frac{y_{j,i}^{\exp} - y_{j,i}^{cal}}{y_{j,i}^{\exp}} \right| \right] \tag{30}$$

where n is number of components, NDP is the number of data points, $x_{j,i}^{\exp}$ and $x_{j,i}^{cal}$ are the measured and calculated mole fraction of H_2S or H_2O in the aqueous phase, respectively, $y_{j,i}^{\exp}$ and $y_{j,i}^{\exp}$ are the measured and calculated mole fraction of H_2S or H_2O in the H_2S-rich phase, respectively.

Comparison between the measured and calculated results is analyzed in terms of average absolute percentage deviation (%*AAD*), average absolute deviation (*AAD*) and absolute deviation (*AD*).

$$\%AAD = \frac{100}{NDP} \sum_{i=1}^{NDP} \left| \frac{z_{\exp,i} - z_{cal,i}}{z_{\exp,i}} \right| \tag{31}$$

$$AAD = \frac{1}{NDP} \sum_{i=1}^{NDP} \left| z_{\exp,i} - z_{cal,i} \right| \tag{32}$$

$$AD = \left| z_{\exp,i} - z_{cal,i} \right| \tag{33}$$

where z_{exp} and z_{cal} are the measured and calculated mole fraction of H_2S or H_2O in the H_2S-rich phase or the aqueous phase.

2.6 BIP Strategies

The two BIPs (i.e., c and k_{ij}) in the HV mixing rule can be constant values or temperature-dependent functions. In this study, different BIP strategies are tried in order to find out the optimal BIP strategy in the HV mixing rule for H_2S/H_2O mixtures. **Table 3** lists the different strategies used to characterize the two BIPs in the HV mixing rule.

Table 3. Different BIP strategies (c and k_{ij}) in the HV mixing rule tested in this study[a]

Case #	BIP Strategy	Description
1	c=constant, k_{ij} =constant	Both c and k_{ij} are determined as constant values over the entire temperature range[b].
2	c=constant, k_{ij} =varying constant	c is optimized as a constant value over the entire temperature range[b], while k_{ij} is optimized at each temperature [c].
3	c=constant, k_{ij} =$k_{ij}(T)$	c is optimized as a constant over the entire temperature range[b], while k_{ij} is first optimized at each temperature and then regressed as a linear function of temperature.
4	c=constant, k_{ij} =$k_{ij}(T^2)$	c is optimized as a constant over the entire temperature range[b], while k_{ij} is first optimized at each temperature and then regressed as a quadratic function of temperature.

a: In this work, the BIP strategies used in this study are similar to the BIP strategies used by Abudour *et al.*[29]

b: The BIP is determined by global optimization: only one BIP value is optimized as a constant for all temperatures that minimizes the objective function. There is only one single BIP value for all temperatures.
c: The BIP values are determined by discrete optimizations: a specific value of BIP is optimized at each temperature to minimize the objective function. The BIP values vary with temperature and appear to be scattered values.

As seen in **Table 3**, four different cases are considered:

- Case 1 represents the basic model. We set both c and k_{ij} as a pair of constants for all temperatures. In this case, c and k_{ij} are temperature independent**.**
- In Case 2, c is determined as a constant (similar to Case 1), while k_{ij} is optimized as a single separate value for each isotherm. When implementing Case 2, we find that c seems to be not dependent on temperature, while k_{ij} tends to show a clear temperature-dependence behavior. Hence, both linear and quadratic relationship between k_{ij} and temperature are explored for further investigation (Cases 3 and 4).
- Cases 3 and 4 are the same as Case 2 except they employ regressed temperature-dependent expressions for BIP instead of using discrete BIP values at different isotherms. As for Case 3, k_{ij} is regressed as a linear function of temperature whereas c is kept as a constant. Using the same c value as used in Case 3, Case 4 employs a quadratic relationship between k_{ij} and temperature. All the values and expressions of BIPs in each case are obtained based on the objective functions defined by equations 28-30.

2.7 Two-Phase Flash Calculations

The two-phase flash calculations in this work are conducted using an in-house Matlab code. When a two phase reaches equilibrium, the two phases should have the same chemical potential as well as the same fugacity coefficient. If a given two phases are in equilibrium at given temperature and pressure, the following relationship holds:

$$f_{Li} = f_{Vi}, i = 1,...,n \tag{34}$$

where f_{Li} and f_{Vi} are the fugacity coefficients of the ith component in liquid phase and vapor phase, respectively.

The key steps of the two-phase flash calculation include K-value (equilibrium ratio) initialization, solution of the Rachford-Rice equation[30], and successive iterations for the solution of K-values. The K-value is defined as:

$$K_i = \frac{y_i}{x_i}, i = 1,...,n \tag{35}$$

where K_i is the equilibrium ratio of the ith component, x_i and y_i are the mole fractions of the ith component in liquid phase and vapor phase, respectively.

Two-phase flash calculation is normally initialized with estimated K-values. The most commonly used K-value initialization method is the one proposed by Wilson[31]:

$$K_i = \frac{\exp\left[5.37\left(1+\omega_i\right)\left(1-T_{ri}^{-1}\right)\right]}{P_{ri}}, i = 1,...,n \tag{36}$$

where ω_i is the acentric factor of the ith component, T_{ri} and P_{ri} are the reduced temperature and pressure of the ith component, respectively.

The Rachford-Rice equation[30] is used to solve the vapor phase faction in two-phase flash calculations:

$$\sum_{i=1}^{n} \frac{z_i(K_i - 1)}{1 + F_v(K_i - 1)} = 0 \tag{37}$$

where z_i is the feed fraction of the ith component, and F_v is the vapor phase fraction. A detailed discussion on the algorithm of the two-flash calculation procedures can be found in the monograph written by Whitson and Brulé[32].

References

[1] Peng, D. Y.; Robinson, D. B. A New Two-Constant Equation of State. *Ind. Eng. Chem. Fundam.* **1976**, *15*, 59–64.

[2] Twu, C. H.; Bluck, D.; Cunningham, J. R.; Coon, J. E. A Cubic Equation of State with a New Alpha Function and a New Mixing Rule. *Fluid Phase Equilib*. **1991**, *69*, 33-50.

[3] Lindeloff, N.; Michelsen, M. L. Phase Envelope Calculations for Hydrocarbon-Water Mixtures. *SPE J*. **2003**, *8*, 298-303.

[4] Martinez, A. P.; Guennec, Y. L.; Privat, R.; Jaubert, J. N.; Mathias, P. M. Analysis of the Combinations of Property Data that Are Suitable for a Safe Estimation of Consistent Twu α-Function Parameters: Updated Parameter Values for the Translated-Consistent tc-PR and tc-RK Cubic Equations of State. *J. Chem. Eng. Data* **2018**, *63(10)*, 3980-3988.

[5] Huron, M. J.; Vidal, J. New Mixing Rules in Simple Equations of State for Representing Vapour-Liquid Equilibria of Strongly Non-Ideal Mixtures. *Fluid Phase Equilib*. **1979**, *3*, 255-271.

[6] Peneloux, A.; Rauzy, E.; Freze, R. A Consistent Correction for Redlich-Kwong-Soave Volume. *Fluid Phase Equilib*. **1982**, *8*, 7-23.

[7] Wong, D. S. H.; Sandler, S. I. A. Theoretically Correct Mixing Rule for Cubic Equation of State. *AIChE J*. **1992**, *5*, 671-680.

[8] Abudour, A. M.; Mohammad, S. A.; Robinson Jr, R. L.; Khaled, A. M. G. Volume-Translated Peng-Robinson Equation of State for Liquid Densities of Diverse Binary Mixtures. *Fluid Phase Equilib*. **2013**, *349*, 37-55.

[9] Chou, G. F.; Prausnitz, J. M. A Phenomenological Correction to an Equation of State for the Critical Region. *AIChE J*. **1989**, *35*, 1487-1496.

[10] Wright, R. H.; Maass, O. The Solubility of Hydrogen Sulphide in Water from the Vapor Pressures of the Solutions. *Can. J. Res*. **1932**, *6*, 94-101.

[11] Selleck, F. T.; Carmichael, L. T.; Sage, B. H. Phase Behavior in the Hydrogen Sulfide-Water System. *Ind. Eng. Chem*. **1952**, *44*, 2219-2226.

[12] Burgess, M. P.; Germann, R. P. Physical Properties of Hydrogen Sulfide-Water Mixtures. *AIChE J*. **1969**, *2*, 272-275.

[13] Clarke, E. C. W.; Glew, D. N. Aqueous Nonelectrolyte Solutions. Part VIII. Deuterium and Hydrogen Sulfides Solubilities in Deuterium Oxide and Water. *Can. J. Chem*. **1971**, *49*, 691-698.

[14] Lee, J. L.; Mather, A. E. Solubility of Hydrogen Sulfide in Water. *Ber. Bunsenges. Phys. Chem*. **1977**, *81*, 1020-1023.

[15] Drummond, S. E. Boiling and Mixing of Hydrothermal Fluids: Chemical Effects on Mineral Precipitation. *Ph. D. Dissertation. Geoscience. Pennsylvania State University* **1981**.

[16] Gillespie, P. C.; Owens, J. L.; Wilson, G. M. Sour Water Equilibria Extended to High Temperatures and with Inerts Present. *AIChE Winter Mtg*., *Atlanta, GA*. **1984**.

[17] Barrett, T. J.; Anderson, G.; Lugowski, M. J. The Solubility of Hydrogen Sulphide in 0–5 m NaCl Solutions at 25–95 C and One Atmosphere. *Geoch. Cosm. Acta*. **1988**, *52*, 807-811.

[18] Carroll, J. J.; Mather, A. E. Phase Equilibrium in the System Water-Hydrogen Sulphide: Modelling the Phase Behavior with an Equation of State. *Can. J. Chem. Eng.* **1989**, *57*, 999-1003.

[19] Suleimenov, O. M.; Krupp, R. E. Solubility of Hydrogen Sulfide in Pure Water and in NaCl Solutions, from 20 to 320 ºC and at Saturation Pressures. *Geoch. Cosm. Acta*. **1994**, *58*, 2433-2444.

[20] Kuranov, G.; Rumpf, B.; Smirnova, N. A.; Maurer, G. Solubility of Single Gases Carbon Dioxide and Hydrogen Sulfide in Aqueous Solutions of N-methyldiethanolamine in the Temperature Range 313−413 K at Pressures up to 5 MPa. *Ind. Eng. Chem. Res*. **1996**, *35*, 1959-1966.

[21] Chapoy, A.; Mohammadi, A. H.; Tohidi, B.; Valtz, A.; Richon, D. Experimental Measurement and Phase Behavior Modeling of Hydrogen Sulfide−Water Binary System. *Ind. Eng. Chem. Res.* **2005**, *44*, 7567-7574.

[22] Koschel, D.; Coxam, J. Y.; Majer, V. Enthalpy and Solubility Data of H_2S in Water at Conditions of Interest for Geological Sequestration. *Ind. Eng. Chem. Res*. **2007**, *46*, 1421-1430.

[23] Savary, V.; Berger, G.; Dubois, M.; Lacharpagne, J. C.; Pages, A.; Thibeau, S.; Lescanne, M. The Solubility of CO_2+H_2S Mixtures in Water and 2 M NaCl at 120°C and Pressures up to 35 MPa. *Int. J. Greenh. Gas Cont*. **2012**, *10*, 123-133.

[24] Clark, S. P. Handbook of Physical Constants. *Geol. Soc*. **1966**.

[25] Murphy, J. A.; Gaines Jr, G. L. Density and Viscosity of Aqueous Hydrogen Sulfide Solutions at Pressures to 20 atm. *J. Chem. Eng. Data* **1974**, *19*, 359-362.

[26] Wood, R. H.; Majer, V. Volumes of Aqueous Solutions of CH_4, CO_2, H_2S and NH_3 at Temperatures from 298.15 K to 705 K and Pressures to 35 MPa. *J. Chem. Thermodyn*. **1996**, *28*, 125-142.

[27] Zhao, H.; Fang, Z.; Jing, H.; Liu, J. Modeling Vapor-Liquid Phase Equilibria of Hydrogen Sulfide and Water System Using a Cubic EOS-G^{EX} Model. *Fluid Phase Equilib.* **2019**, *484*, 60-73.

[28] Duan, Z.; Sun, R.; Liu, R.; Zhu, C. Accurate Thermodynamic Model for the Calculation of H_2S Solubility in Pure Water and Brines. *Energy Fuels* **2007**, *21*, 2056-2065.

[29] Abudour, A. M.; Sayee, A. M.; Khaled, A. M. G. Modeling High-Pressure Phase Equilibria of Coalbed Gases/Water Mixtures with the Peng–Robinson Equation of State. *Fluid Phase Equilib.* **2012**, *319*, 77-89.

[30] Rachford Jr, H. H.; Rice, J. D. Procedure for Use of Electronic Digital Computers in Calculating Flash Vaporization Hydrocarbon Equilibrium. *J. Pet. Technol*. **1952**, *410*, 19-3.

[31] Wilson, G. M. A Modified Redlich-Kwong Equation of State, Application to General Physical Data Calculations. *65th National AIChE Meeting, Cleveland,* **1969***,15*.

[32] Whitson, C. H.; Brulé, M. R. Phase Behavior (Vol. 20). Richardson, TX: Henry L. Doherty Memorial Fund of AIME. *SPE*. **2000**.

CHAPTER 3 RESULTS AND DISCUSSION

3.1 Determination of the Optimal BIP Strategy

Table 4 shows the performance of the different BIP strategies in reproducing the measured VLE/LLE data for H_2S/H_2O mixtures. The results are presented using error indices *%AAD* and *AAD* for H_2O's mole fraction in the H_2S-rich phase (denoted as y_1) and H_2S's mole fraction in the aqueous phase (denoted as x_2). Since the values of y_1 and x_2 are very small in the H_2S/H_2O binary system, small absolute errors in these mole fractions may lead to large values in percentage errors. Therefore, we provide both *%AAD* and *AAD* values for comparison purpose. As mentioned previously, the measured data reported by Selleck *et al.*[1] at pressures above 100 bar are not reliable. Therefore, we do not consider these data in *%AAD* and *AAD* calculations. **Table 5** shows the coefficients of k_{ij} correlations regressed in Case 3 (linear correlation) and Case 4 (quadratic correlation).

Table 4. *%AAD* and *AAD* of calculated H_2O's mole fraction in the vapor phase (y_1) and H_2S's mole fraction in the aqueous phase (x_2) by different BIP strategies[a]

Case #	BIP Strategy	H_2O's Mole Fraction in H_2S-Rich Phase (y_1)		H_2S's Mole Fraction in Aqueous Phase (x_2)	
		%AAD	$AAD\times10^3$	*%AAD*	$AAD\times10^3$
1	c=0.088, k_{ij} =0.172	6.52	3.63	15.80	1.32
2	c=0.016, k_{ij} =varying constant	-	-	-	-
3	c=0.016, $k_{ij} = k_{ij}(T)$ (See **Table 5** for the detailed expression)	4.90	3.48	4.95	0.89
4	c=0.016, $k_{ij} = k_{ij}(T^2)$ (See **Table 5** for the detailed expression)	5.68	4.72	7.72	1.09

a: Due to the large deviation from measured data and modelling results, the measured data reported by Selleck *et al.*[1] (only above 100 bar) are not considered for *%AAD* and *AAD* analysis.

Table 5. Coefficients of the linear temperature-dependence equation for k_{ij} in Case 3 and the quadratic temperature-dependence equation for k_{ij} in Case 4.

Case #	$k_{ij}=AT+B$			
3	$T \leq 350$ K		$T > 350$ K	
	A	*B*	*A*	*B*
	9.99E-04	-3.00E-01	5.54E-04	-1.50E-01
4	$k_{ij}=AT^2+BT+C$			
	A	*B*	*C*	
	-1.77E-06	2.00E-03	-4.41E-01	

As seen from Table 4, a pair of constant BIPs shows a very good accuracy in reproducing H_2O's mole fraction in H_2S-rich phase (y_1). However, Case 1 BIP strategy leads to a relatively large error in reproducing H_2S's mole fraction in the aqueous phase (x_2); it yields an *%AAD* of 15.80% in x_2 calculations.

As for Case 2, c is optimized as 0.016 over the entire temperature range and k_{ij} is determined by the individualized optimization for each isotherm as explained in **Table 3**. The reason why we do not show the accuracy of Case 2 is that the varying k_{ij} values are not in the form of any generalized expression (i.e., they are individual values for each isotherm). Therefore, it is pointless to discuss the accuracy offered by Case 2 if k_{ij} cannot be generalized as a function of temperature. Besides, Case 2 is designed for obtaining the temperature-dependent BIP expressions. Unfortunately, we could not find any relationship between c values and temperature when k_{ij} is optimized at each isotherm. The temperature dependences of c and k_{ij} in Case 2 are shown in **Figure 1** and **Figure 2**, respectively.

In Case 3, k_{ij} is regressed as a linear function of temperature (as shown in **Table 5**) along with a constant c with the value of 0.016. As we can see from **Table 4**, Case 3 improves the accuracy of x_2 prediction by more than 65% as compared to Case 1; however, it offers a similar accuracy in calculating H_2O solubility in the H_2S-rich phase. In other words, there is no dramatic

improvement in predicting y_1 by the generalized temperature-dependent k_{ij} correlation. The red sloid lines in **Figure 2** are the linear relations regressed based on the individual k_{ij} values. One interesting observation from **Figure 2** is that the optimized k_{ij} values tend to exhibit two linear trends at temperatures lower and higher than 350 K. Therefore, k_{ij} is regressed using two linear relations; the regressed equations are shown in **Table 5**. As shown in **Table 5**, we employ a quadratic function in Case 4 to describe the relationship between k_{ij} and temperature instead of the linear one in Case 3. The results show that using a quadratic relationship between k_{ij} and temperature is not capable of improving the accuracy of mutual solubility calculations in either phase. Therefore, in view of its accuracy and simplicity, Case 3 can be considered as the best BIP strategy among all the cases shown in **Table 3.**

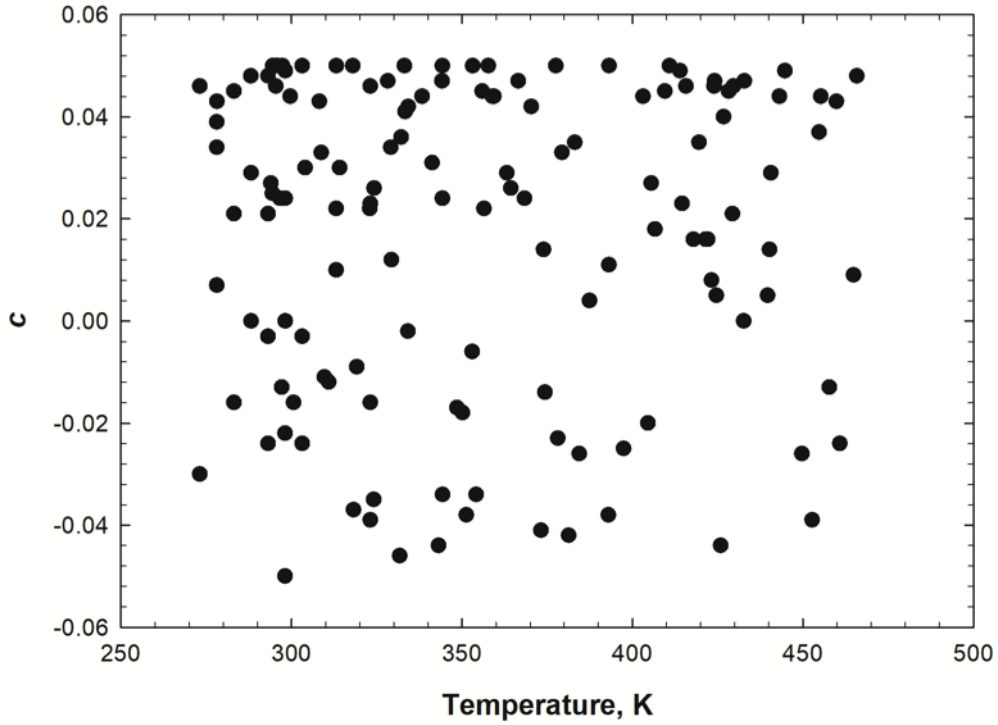

Figure 1. Relationship between optimized *c* and temperature in Case 2.

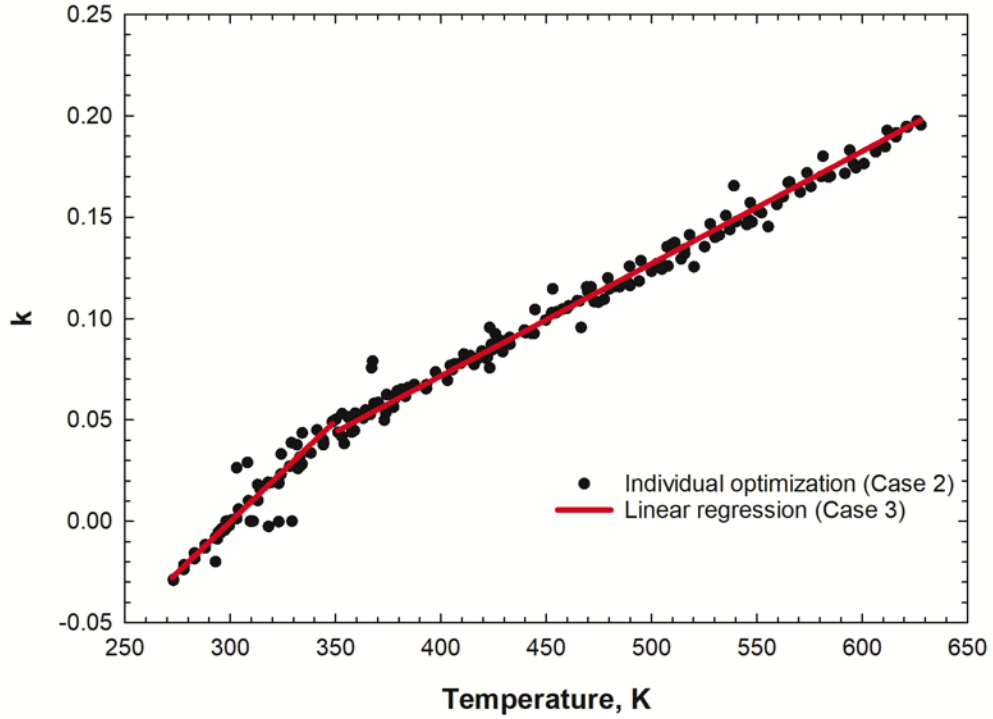

Figure 2. Plot of optimized k_{ij} values versus temperature in Case 2 and Case 3.

As discussed previously, we present all the calculation results in terms of the errors for the lower-solubility components in each phase (e.g., *%AAD* for y_1 and x_2). Thus, the percentage deviations may appear to be large because of the small values of mole fractions of these components. Therefore, it is necessary and meaningful to show the *ADs* between the measured data and modelling results. Here, we only present the *AD* against temperature and pressure for Case 3 for simplicity. **Figures 3a and 3b** graphically show the *AD* distributions for Case 3 as functions of temperature (a) and pressure (b), respectively. **Figure 3** demonstrates that the EOS model coupled with Case 3 BIP strategy is capable of precisely reproducing the mutual solubility in both phases (most of *AD* values in **Figure 3** are below 10^{-3}). Also, we can see from **Figure 3** that x_2 prediction appears to be more accurate than y_1 prediction. Hence, Case 3 BIP strategy allows for reasonable and accurate reproduction of VLE/LLE for H_2S/H_2O mixtures in the temperature and pressure range considered in this work.

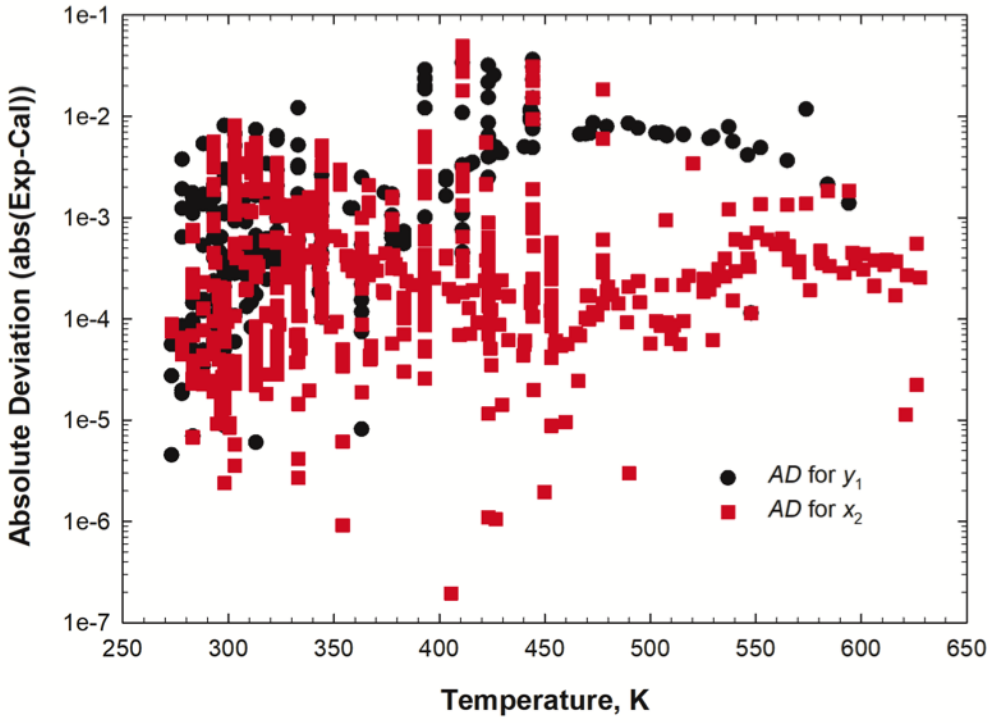

(a)

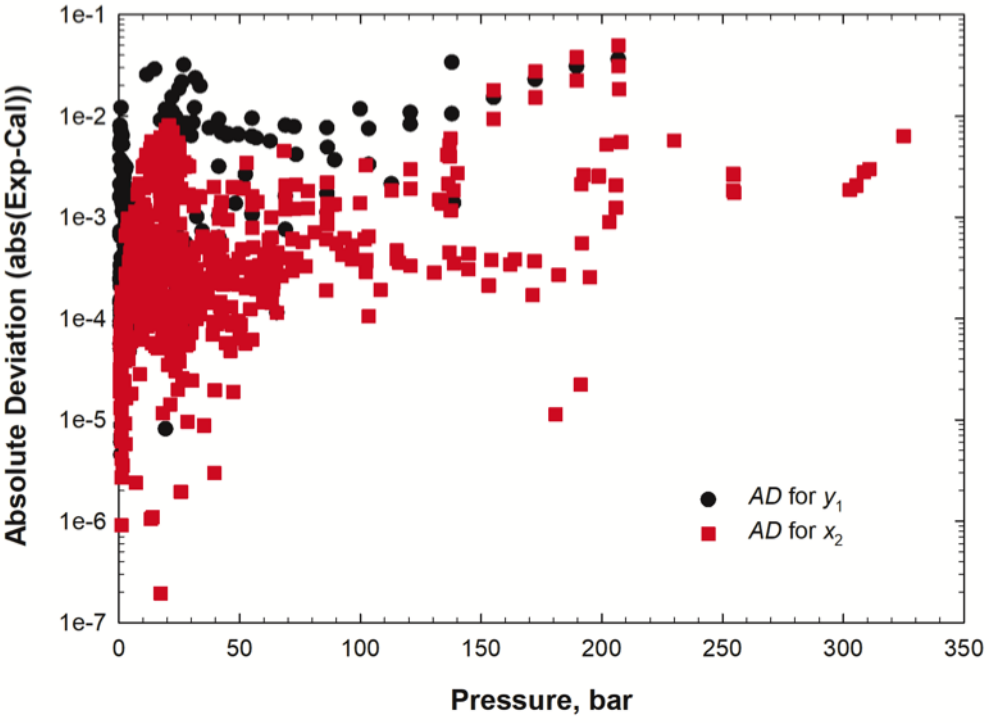

(b)

Figure 3. Plots of *ADs* for y_1 and x_2 prediction versus temperature (a) and pressure (b) yielded by the EOS model coupled with Case 3 BIP strategy.

3.2 Performance of the Optimal BIP Strategy in Reproducing VLE/LLE Data

3.2.1 H_2O Solubility in the H_2S-rich Phase (y_1)

In this section, the comparison between Case 1 and Case 3 in y_1 prediction is demonstrated and discussed. **Figure 4** and **Figure 5** show the results of y_1 prediction for Case 1 (denoted as Twu-HV-1) and Case 3 (denoted as Twu-HV-2), respectively. In general, these two models have similar accuracy in computing H_2O solubility in the H_2S-rich phase.

At low and medium temperatures (See **Figure 4a** and **Figure 5a**), both Case 1 and Case 3 present almost identical results. Over this temperature range of 273.15-344.26 K, both two cases are able to accurately model the phase behavior of H_2S/H_2O system at pressures up to 10 bar. Over the temperature range of 303.15-344.26 K (See **Figure 4b** and **Figure 5b**), H_2O's solubility calculated by Case 1 and 3 show abrupt changes at pressures above 20 bar. These sharp changes can be attributed to the change from VLE to LLE.

Over the temperature range of 359.2-393.2 K (See **Figure 4c** and **Figure 5c**), the calculated H_2O solubility in the H_2S-rich phase calculated by both Case 1 and Case 3 show sudden changes at temperatures around 373 K. Overall, both Case 1 and Case 3 are capable of capturing the variation trend of H_2O solubility in the H_2S-rich phase over the temperature range of 359.2-393.2 K and at pressures up to 70 bar.

As for the temperature range of 403.15-444.26 K (See **Figure 4d** and **Figure 5d**), both models can correlate H_2O's solubility in the H_2S-rich phase up to 100 bar. Over the temperature range of 403.15-423.15 K, the calculated results by Case 3 show a relatively large deviation from the measured data at pressures above 100 bar reported by Selleck *et al.*[1] Previous study[2] suspects that Selleck *et al.*[1] data at pressures higher than 100 bar are not reliable. But Case 1 is somehow

capable of capturing the trend of the measured data reported by Selleck *et al.*[1] Finally, **Figure 4e** and **Figure 5e** show that both Case 1 and Case 3 provide excellent reproduction of the measured data over the temperature range of 466.6-594.15 K and pressures up to 300 bar.

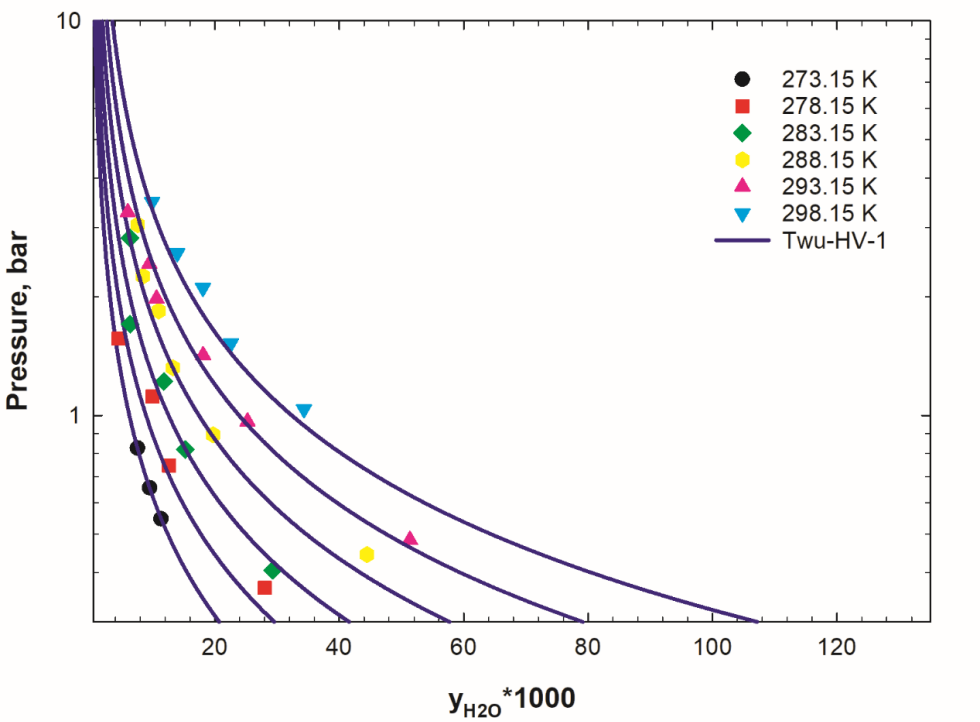

(a)

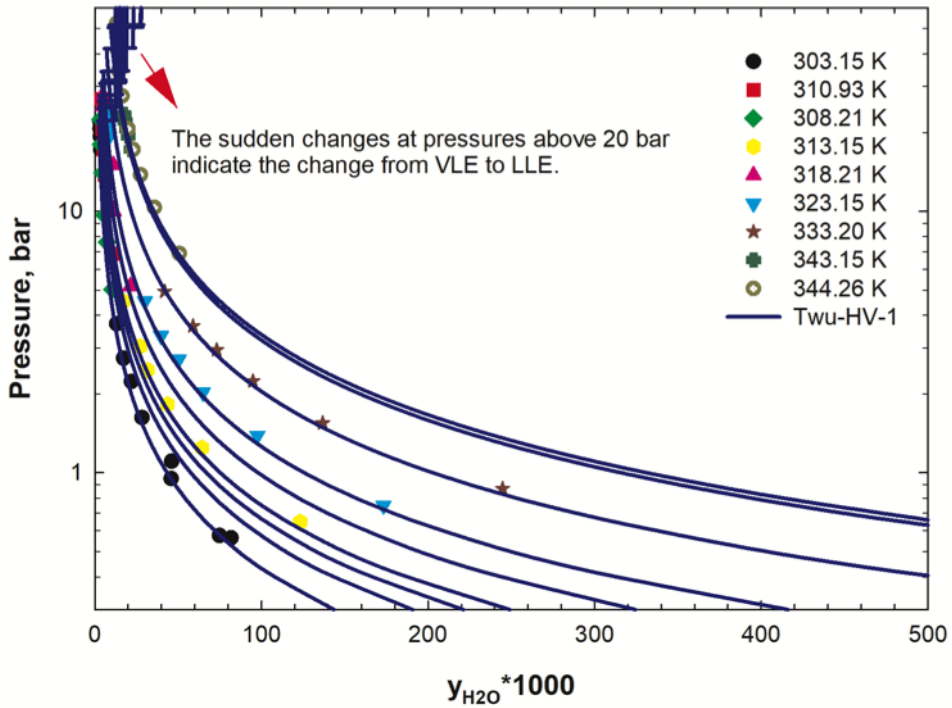
The sudden changes at pressures above 20 bar
indicate the change from VLE to LLE.
303.15 K
310.93 K
308.21 K
313.15 K
318.21 K
323.15 K
333.20 K
343.15 K
344.26 K
Twu-HV-1
Pressure, bar
10
1
0
100
200
300
400
500
y_{H2O}*1000

(b)

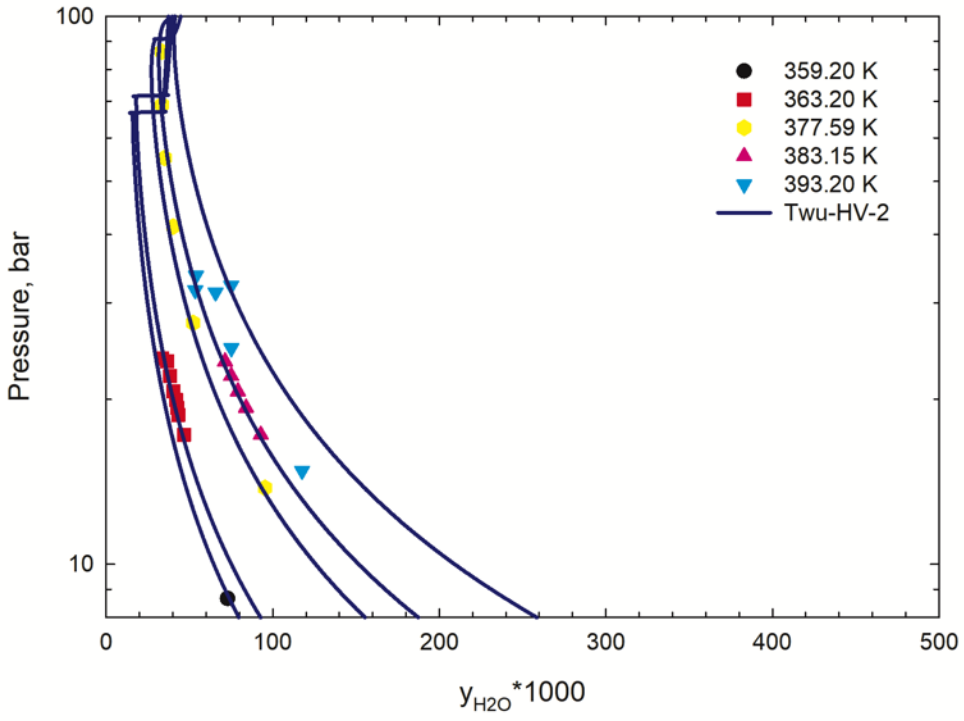
359.20 K
363.20 K
377.59 K
383.15 K
393.20 K
Twu-HV-2
Pressure, bar
100
10
0
100
200
300
400
500
y_{H2O}*1000

(c)

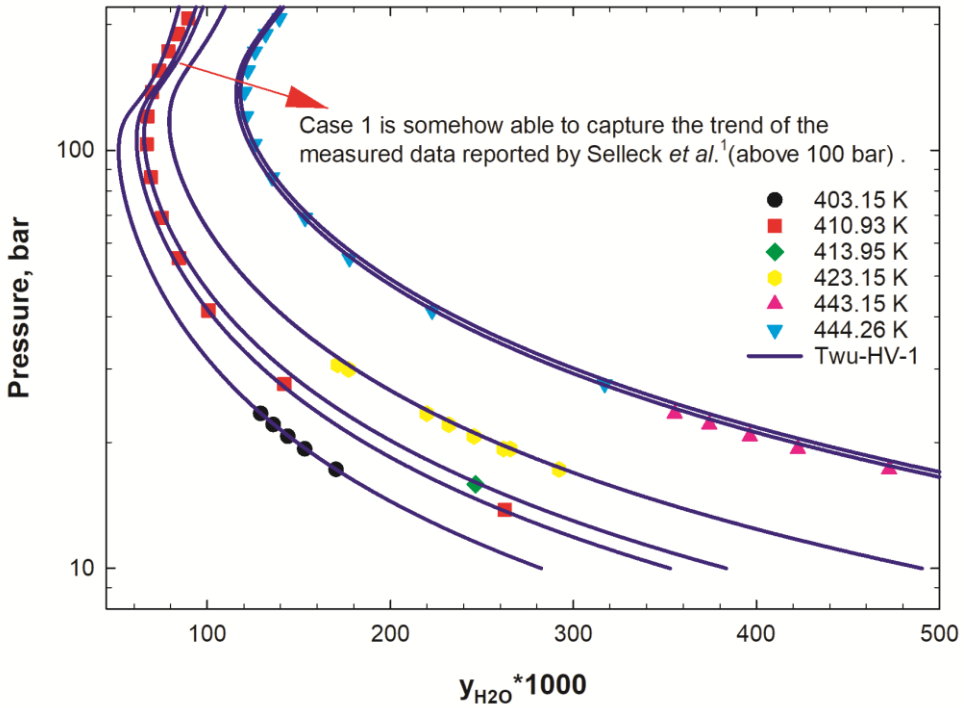

(d)

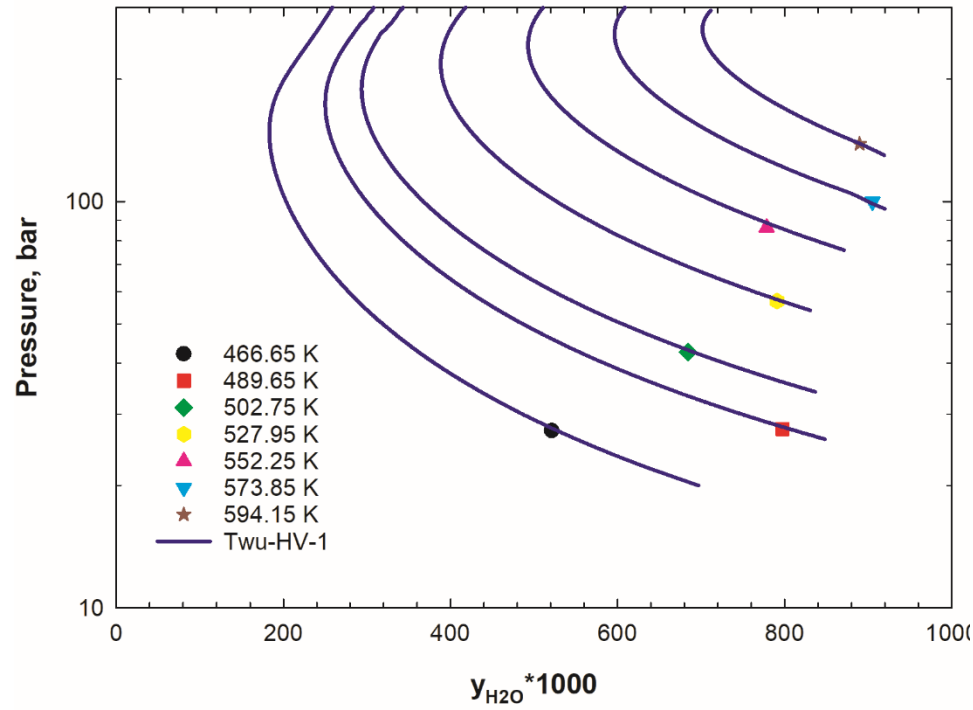

(e)

Figure 4. Reproduction of y_1 (H_2O solubility in the H_2S-rich phase) at 273.15-594.15 K by Case 1 (denoted as Twu-HV-1) (a: 273.15-298.15 K; b: 303.15-344.26 K; c: 359.20-393.20 K; d:

403.15-444.26 K; e: 466.6-594.15 K). Experimental data are taken from several previous studies[3-7, 12, 14].

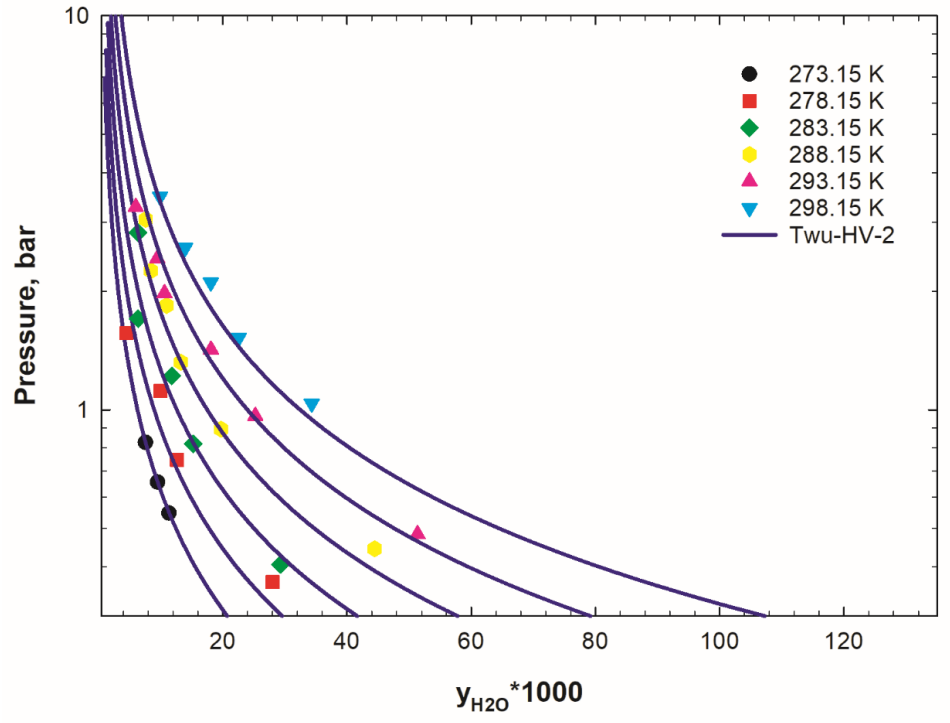

(a)

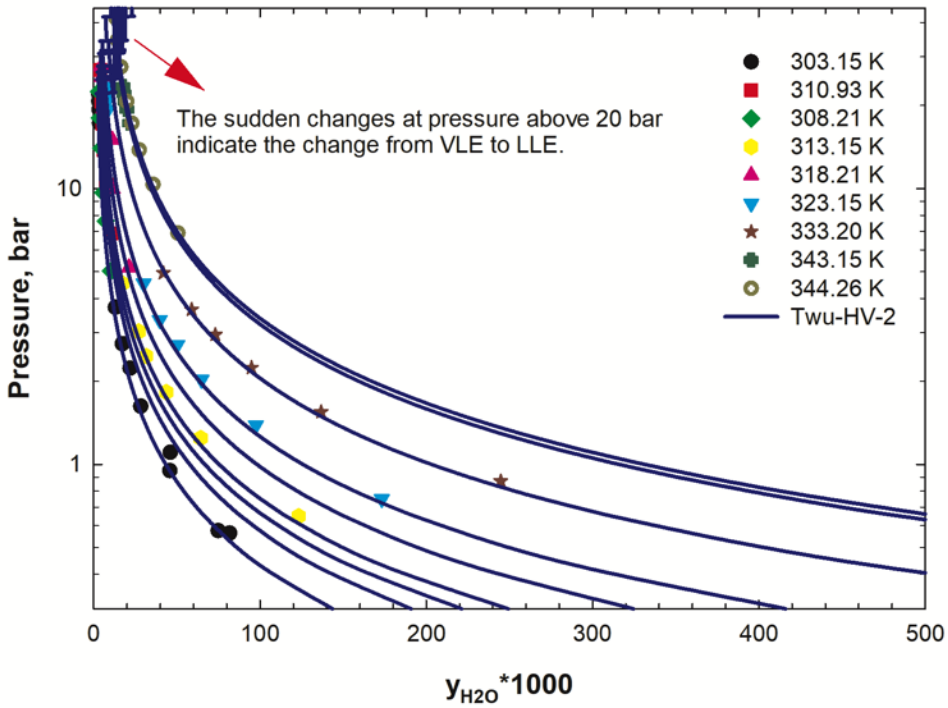

(b)

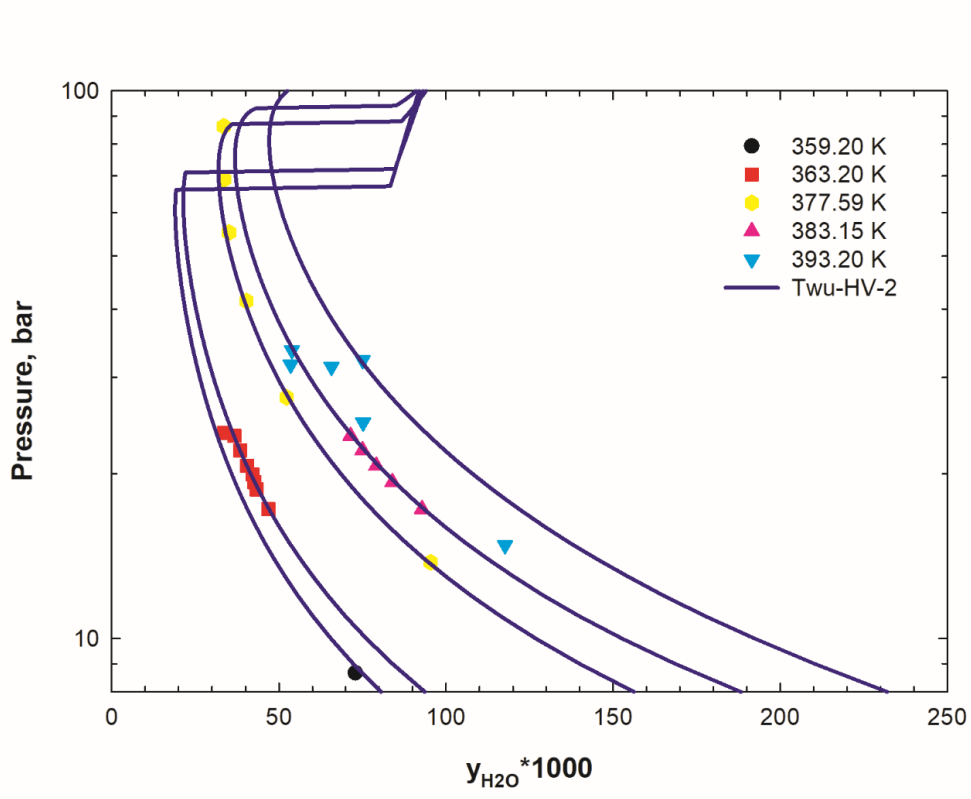
100
10
0
50
100
150
200
250
Pressure, bar
y_{H2O}*1000
359.20 K
363.20 K
377.59 K
383.15 K
393.20 K
Twu-HV-2

(c)

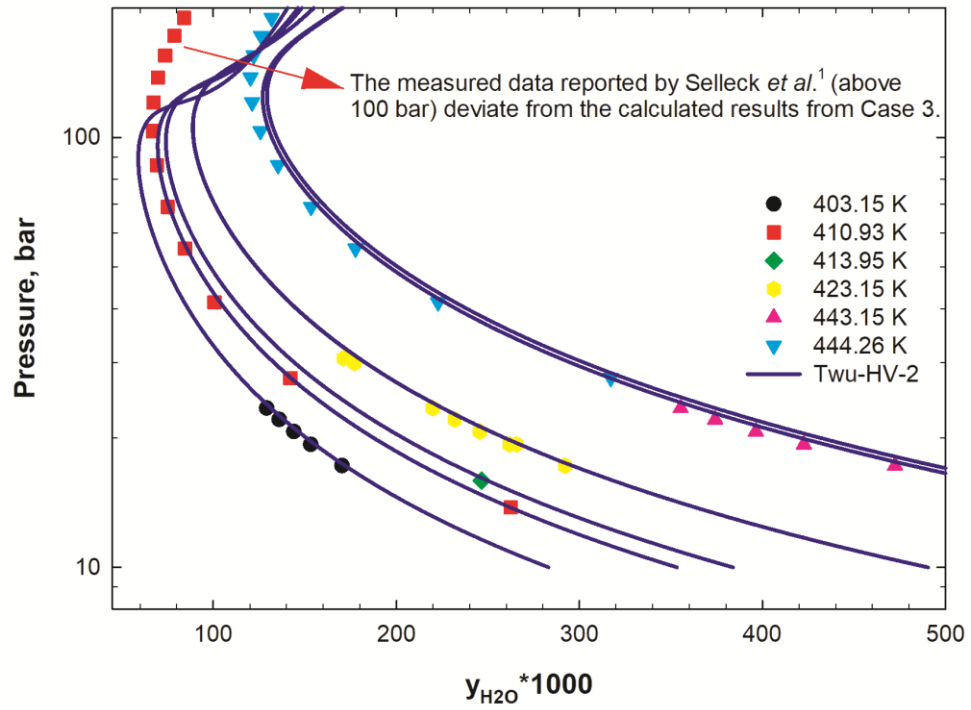
The measured data reported by Selleck *et al.*[1] (above 100 bar) deviate from the calculated results from Case 3.
100
10
100
200
300
400
500
Pressure, bar
y_{H2O}*1000
403.15 K
410.93 K
413.95 K
423.15 K
443.15 K
444.26 K
Twu-HV-2

(d)

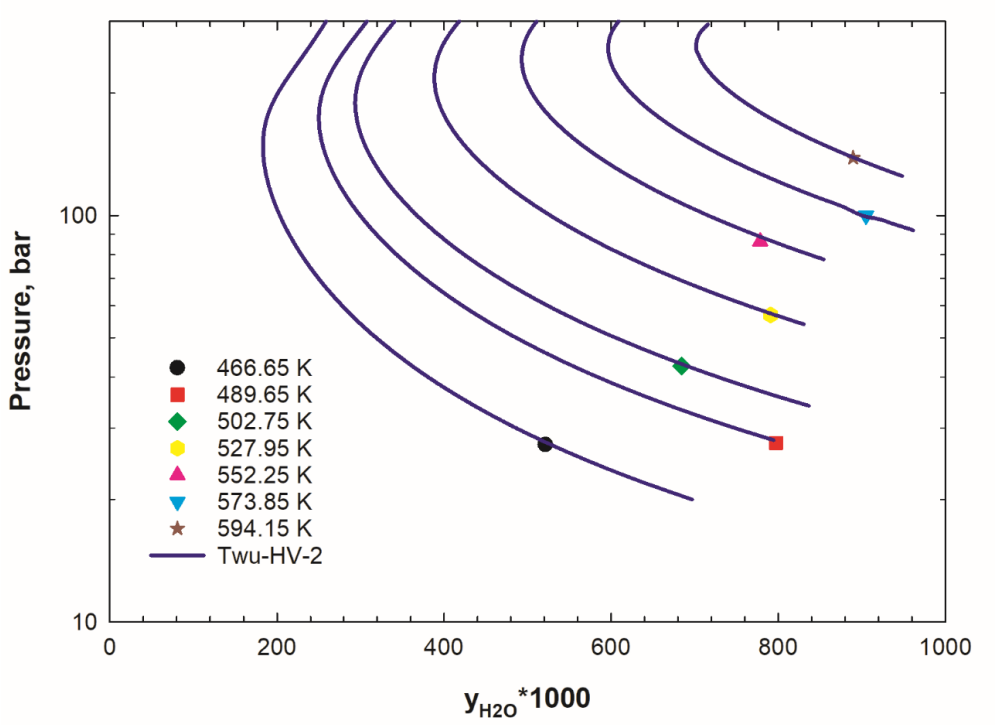

(e)

Figure 5. Reproduction of y_1 (H_2O solubility in the H_2S-rich phase) at 273.15-594.15 K by Case 3 (denoted as Twu-HV-2) (a: 273.15-298.15 K; b: 303.15-344.26 K; c: 359.20-393.20 K; d: 403.15-444.26 K; e: 466.65-594.15 K). Experimental data are taken from several previous studies[3-7, 12, 14].

3.2.2 H_2S Solubility in the Aqueous Phase (x_2)

Figure 6 shows the x_2 calculation results by Case 1, while **Figure 7** shows the x_2 calculation results by Case 3. Comparison of **Figures 6** and **7** reveals that Case 3 gives a much better performance in reproducing the measured data of H_2S's solubility in the aqueous phase than Case 1, which is consistent with the results shown in **Table 4**.

At low temperatures and pressures (See **Figure 6a** and **Figure 7a**), both Case 1 and Case 3 are generally capable of capturing the variation trend of the experimental data in this temperature range at pressures up to 15 bar. However, Case 1 tends to overestimate the H_2S solubility in the aqueous phase, while Case 3 offers a very good agreement between the calculated data and the measure ones.

Over the temperature range of 303.15-344.15 K (See **Figure 6b** and **Figure 7b**), Case 1 gives relatively large errors in computing x_2, while Case 3 gives a much higher accuracy in computing x_2. As labelled in **Figure 6b** and **Figure 7b**, two data points reported by Carroll and Mather[10] (333.15 K, green star) and Clarke and Glew[5] (313.15 K, yellow circle) deviate from the bulk data and calculated results from both cases.

At temperatures of 353-393.15 K (See **Figure 6c and Figure 7c**), both experimental data and modelling results from both cases are experiencing a sudden discontinuity due to the switch from VLE to LLE at the pressure of about 90 bar. In general, over this temperature range, Case 1 tends to underestimate the mole fraction of H_2S in the aqueous phase (as labelled in **Figure 6c**), while Case 3 is capable of accurately estimating the mole fraction of H_2S in the aqueous phase except at 377.59 K and 70+ bar. The experimental data points at 377.59 K (pink triangles) are taken from Selleck *et al.*[1] Their dataset at 70+ bar deviates from both modelling results (Case 1 and Case 3). In addition, the trend exhibited by the Selleck *et al.*[1] data at 377.59 K and 70+ bar tends to be also quite different from the trend exhibited in the experimental data at similar temperatures and pressures reported by Koschel *et al.*[14] and Savary *et al.*[15]

At temperatures of 403.15-477.60 K (See **Figure 6d** and **Figure 7d**), the modelling results from both cases show very good agreement with the experimental data at pressures up to 100 bar, but the calculated results by Case 1 show larger errors than those by Case 3. Again, the experimental data points at the temperatures of 410.93 K (red squares) and 444.26 K (blue triangles) and pressures of 100+ bar taken from Selleck *et al.*[1] deviate from the modelling results by Case 3. Similar to the y_1 prediction in this temperature range, Case 1 can capture the variation trend of the experimental data at the temperature of 444.26 K (blue triangles) and pressures of 100+ bar reported by Selleck *et al.*[1]

At temperatures above 466.65 K (See **Figure 6e** and **7e**), the modeling results from both Case 1 and Case 3 show an excellent agreement with the measured data.

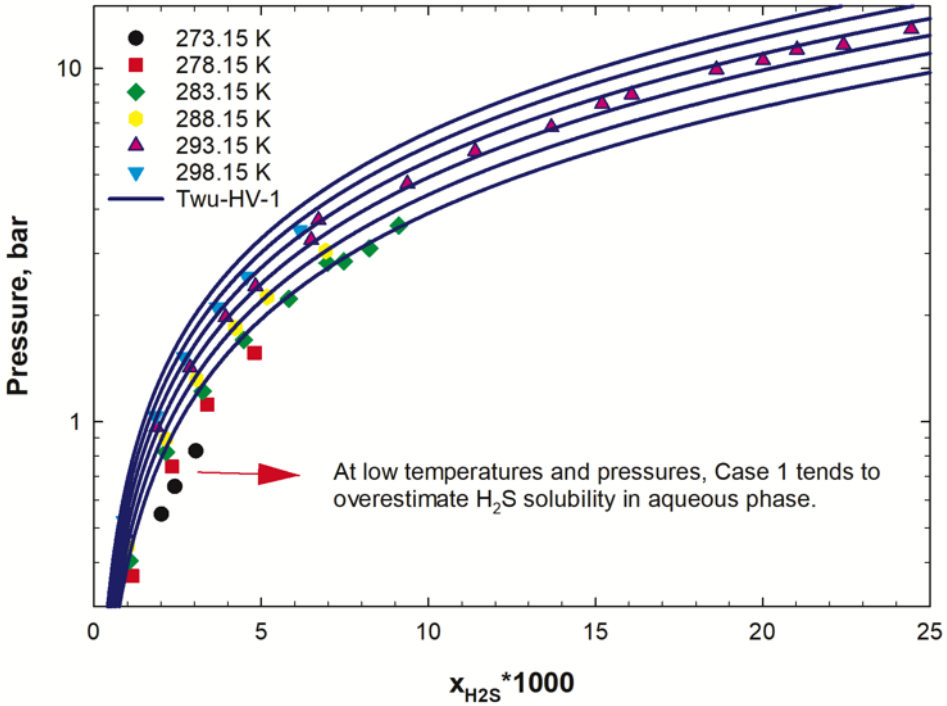

(a)

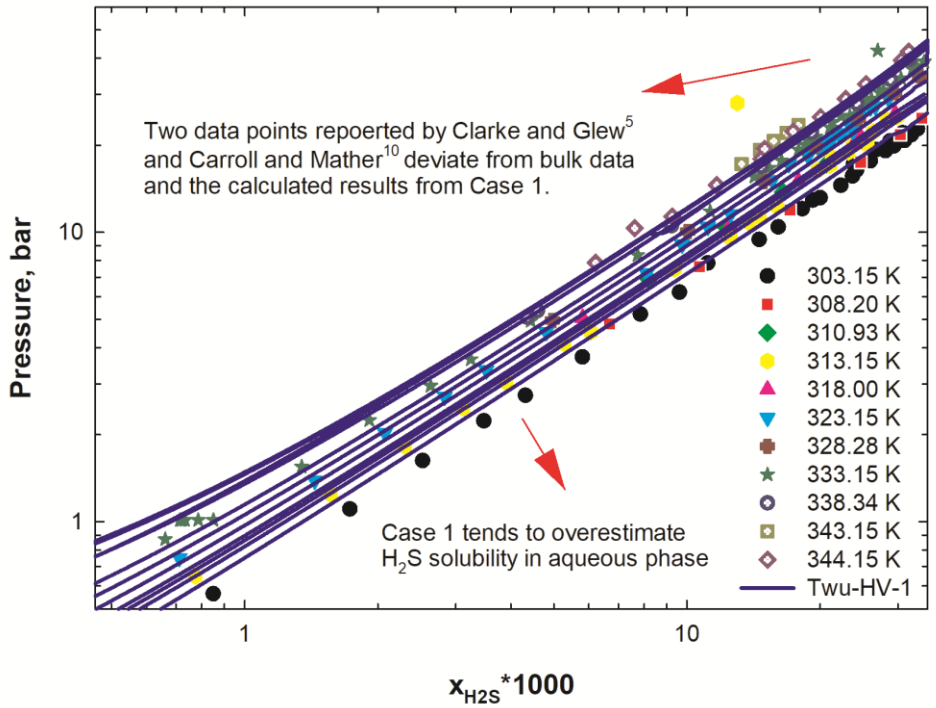
Two data points repoerted by Clarke and Glew[5] and Carroll and Mather[10] deviate from bulk data and the calculated results from Case 1.
Case 1 tends to overestimate H_2S solubility in aqueous phase
303.15 K
308.20 K
310.93 K
313.15 K
318.00 K
323.15 K
328.28 K
333.15 K
338.34 K
343.15 K
344.15 K
Twu-HV-1
Pressure, bar
10
1
1
10
x_{H2S}*1000

(b)

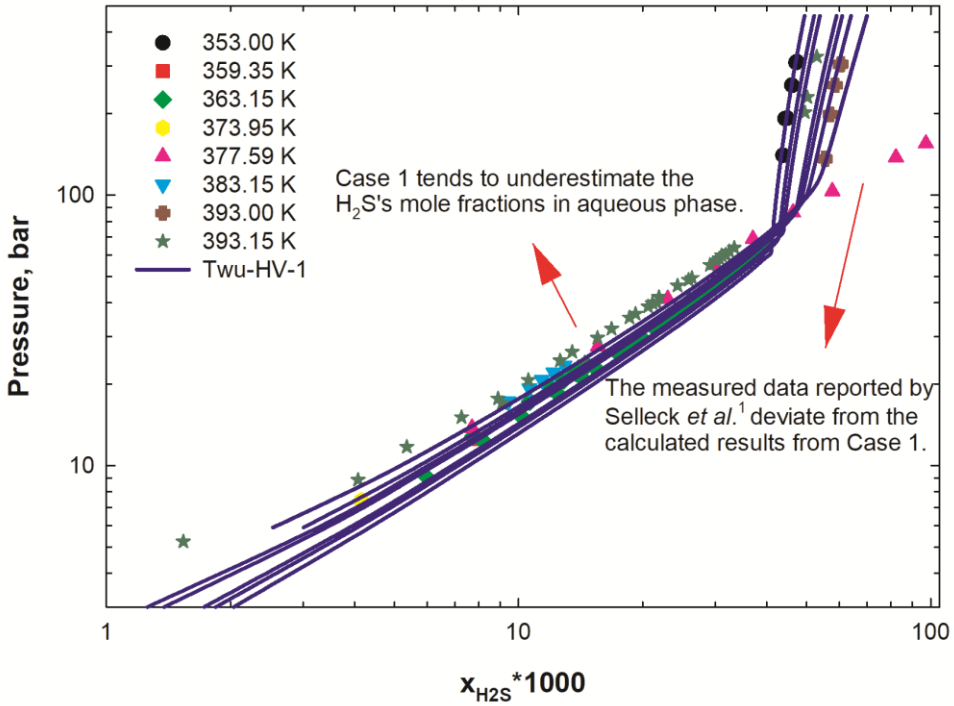
353.00 K
359.35 K
363.15 K
373.95 K
377.59 K
383.15 K
393.00 K
393.15 K
Twu-HV-1
Case 1 tends to underestimate the H_2S's mole fractions in aqueous phase.
The measured data reported by Selleck *et al.*[1] deviate from the calculated results from Case 1.
Pressure, bar
100
10
1
10
100
x_{H2S}*1000

(c)

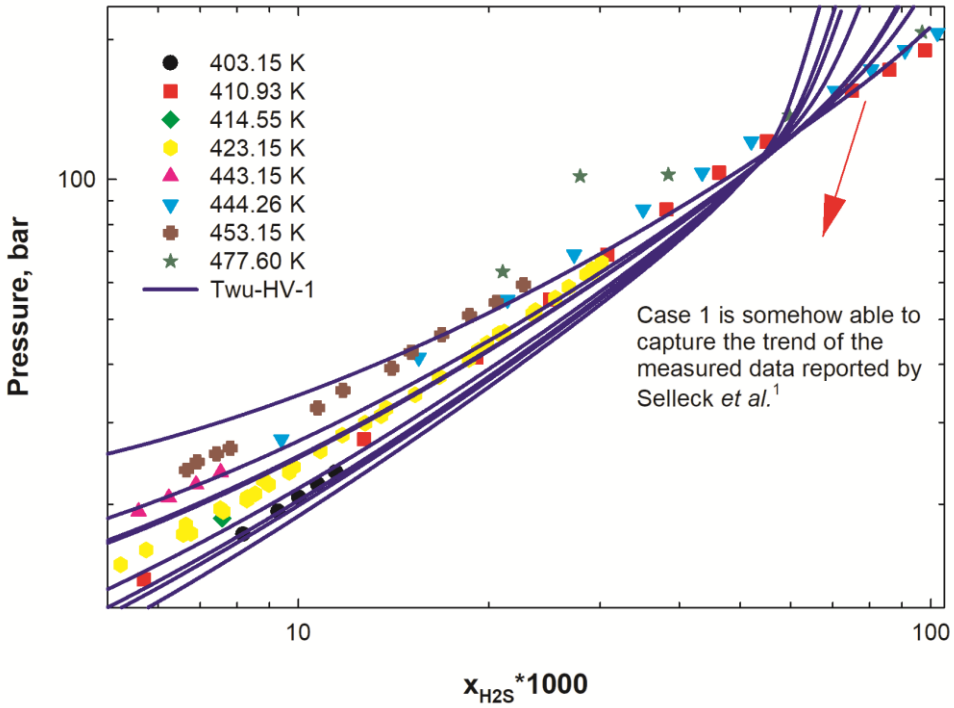

(d)

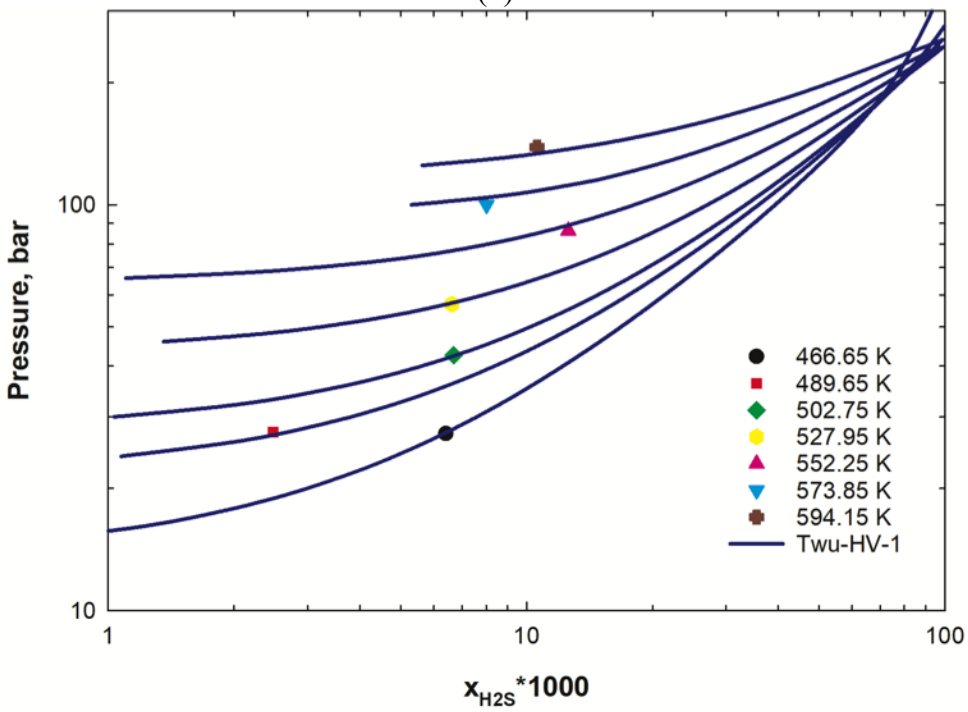

(e)

Figure 6. Reproduction of x_2 (H_2S solubility in the aqueous phase) at 273.15-594.15 K by Case 1 (denoted as Twu-HV-1) (a: 273.15-298.15 K; b: 303.15-344.15 K; c: 353.00-393.15 K; d:

403.15-477.60 K; e: 466.65-594.15 K). Experimental data are taken from several previous studies[1, 3-15].

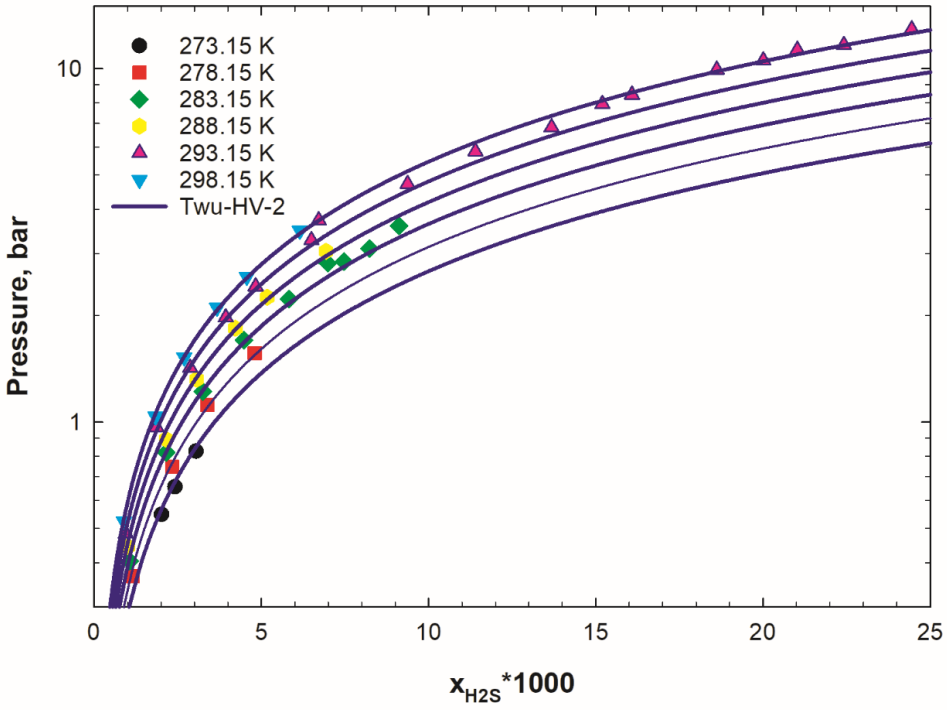

(a)

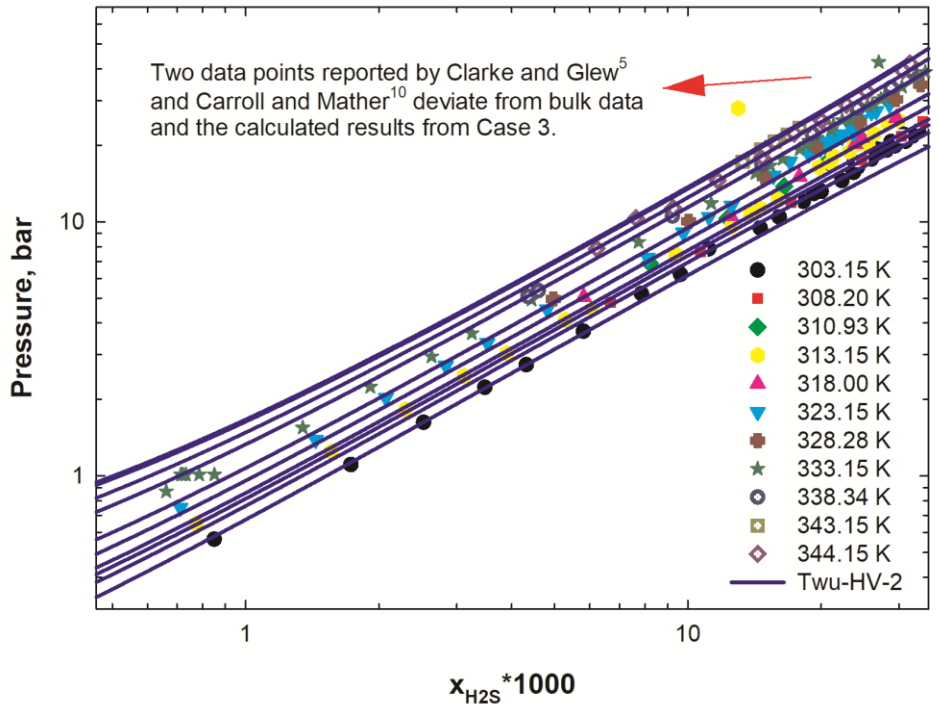

(b)

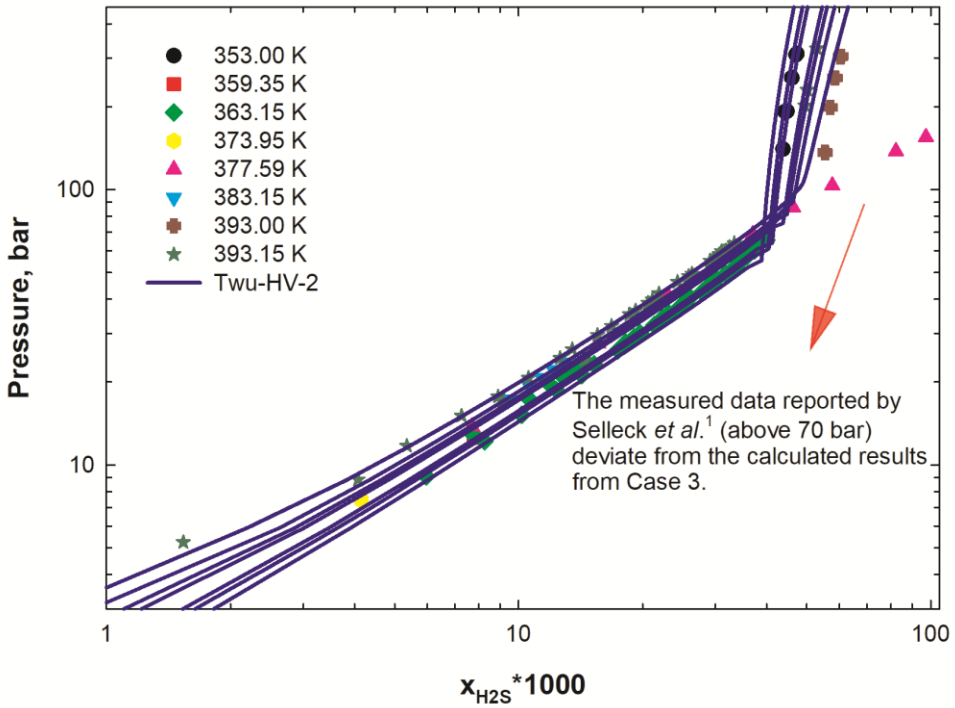
353.00 K
359.35 K
363.15 K
373.95 K
377.59 K
383.15 K
393.00 K
393.15 K
Twu-HV-2
The measured data reported by Selleck et al.[1] (above 70 bar) deviate from the calculated results from Case 3.
Pressure, bar
100
10
1
10
100
x_{H2S}*1000

(c)

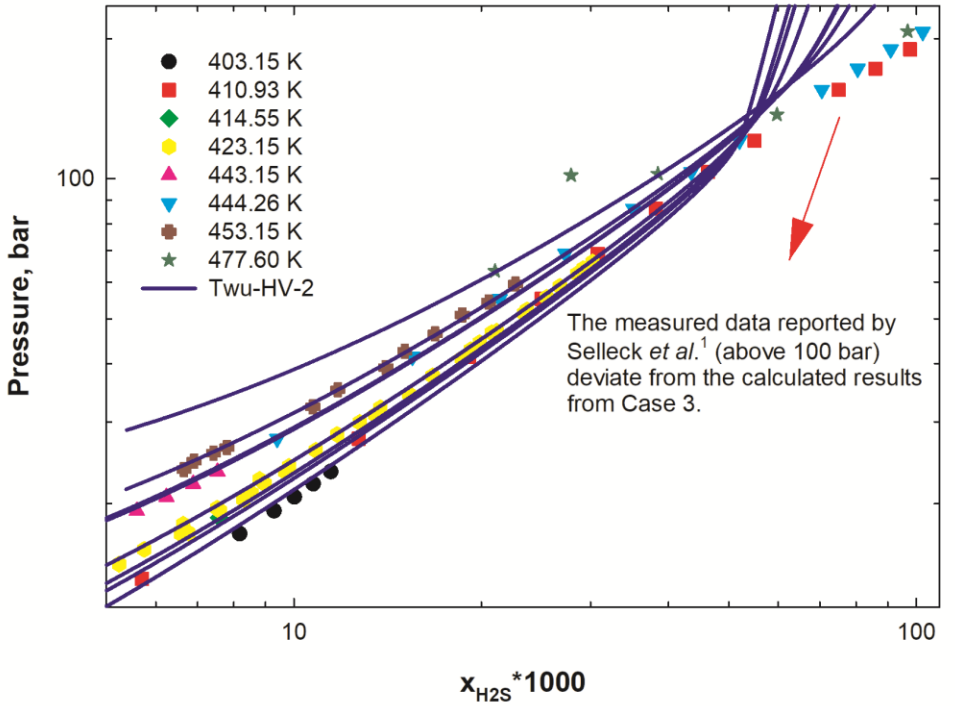
403.15 K
410.93 K
414.55 K
423.15 K
443.15 K
444.26 K
453.15 K
477.60 K
Twu-HV-2
The measured data reported by Selleck et al.[1] (above 100 bar) deviate from the calculated results from Case 3.
Pressure, bar
100
10
100
x_{H2S}*1000

(d)

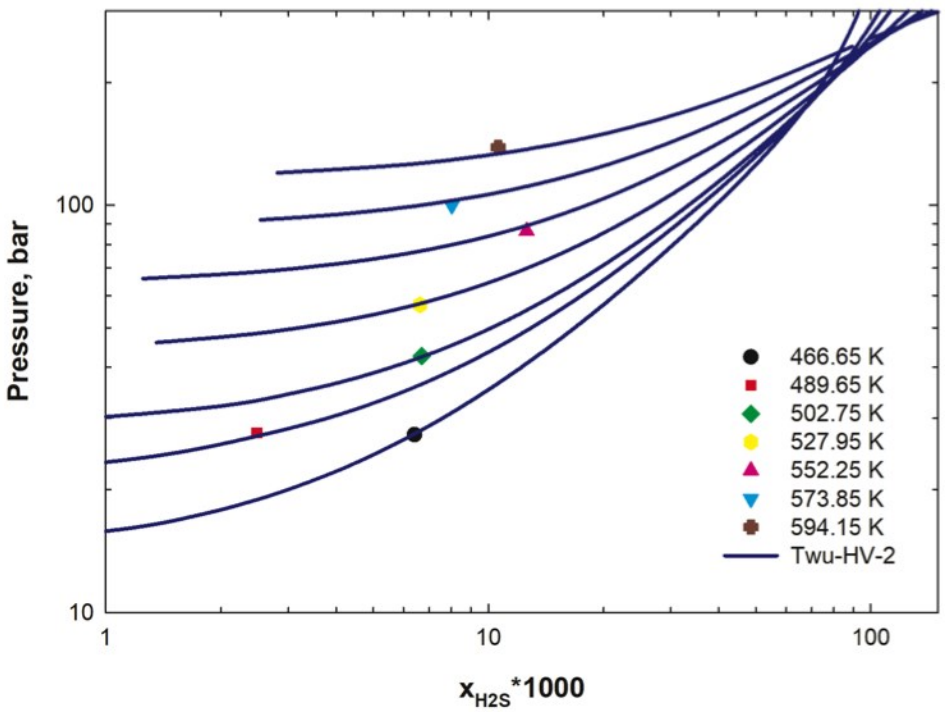

(e)

Figure 7. Reproduction of x_2 (H_2S solubility in the aqueous phase) at 273.15-594.15 K by Case 3 (denoted as Twu-HV-2) (a: 273.15-298.15 K; b: 303.15-344.15 K; c: 353.00-393.15 K; d: 403.15-477.60 K; e: 466.65-594.15 K). Experimental data are taken from several previous studies[1, 3-15].

Figure 8 demonstrates the pressure-composition diagrams of H_2S/H_2O mixtures at high temperatures (529.55-627.85K) calculated from Zhao *et al.*[2] model and the newly developed model by this study. As seen from Figure 8, similar to Zhao *et al.*[2] model, our model is capable of making reliable computations of VLE/LLE for H_2S/H_2O mixtures, although the calculated two-phase envelopes by the two models appear to be quite different, especially at the higher-pressure side of the two-phase envelopes. In general, as the temperature increases, there is shrinkage in the coverage of the two-phase region of H_2S/H_2O mixtures. It is worthwhile nothing that one inherent edge of the newly developed model is that it can be readily applied to VLE/LLE calculations for H_2S/H_2O mixtures. In comparison, one needs to interpolate the BIP values in Zhao *et al.*[2] model prior to its implementation, thus hindering its straightforward application.

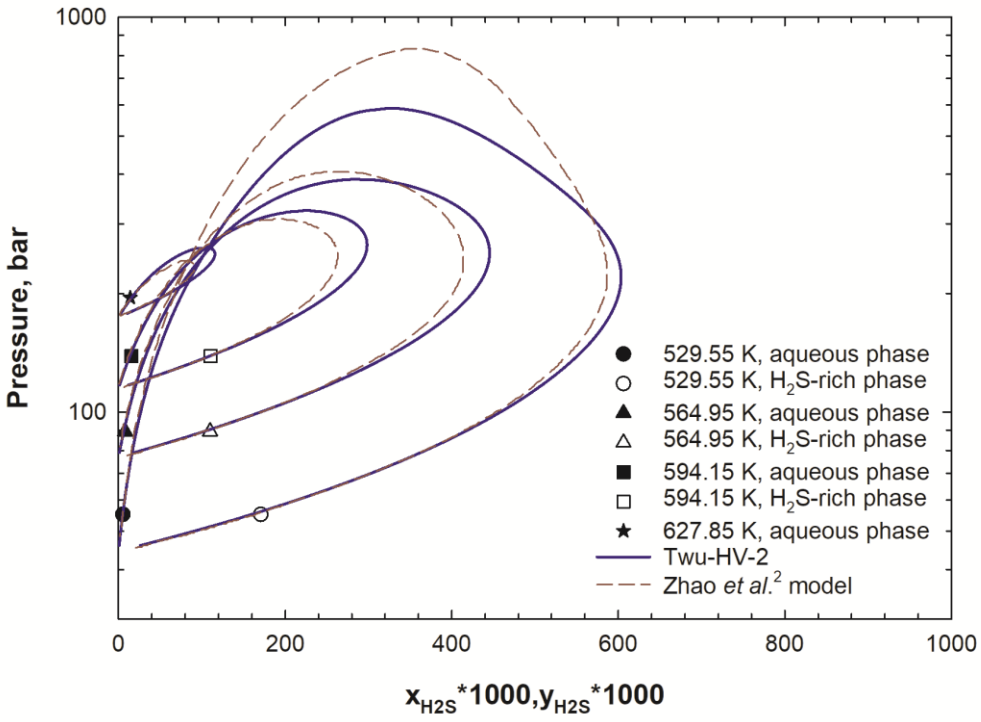

Figure 8. Pressure-composition diagrams of H_2S/H_2O mixtures computed by Zhao *et al.*[2] model and the newly developed model (denoted as Twu-HV-2) at high temperatures (529.55-627.85 K). Experimental data are taken from two previous studies[7, 11].

3.3 Performance of Volume Translated-PR EOS in Predicting Density Data

In this study, more experimental data are collected from the literature[16-18] to examine the performance of the volume-translated PR EOS in predicting density of H_2S/H_2O mixtures. This section demonstrates the capability of Case 3 (i.e., Twu-HV-2) coupled with different volume translation models in estimating density of H_2S/H_2O mixtures. Previously, Zhao *et al.*[2] calculated the total fluid volumes for one H_2S/H_2O mixtures by applying PRSV EOS and WS mixing rule[19] (PRSV+WS) and compared their calculated results to the measured ones[11]. The comparative analysis showed that the modeled volume data yields a relatively large deviation from the measured ones reported by Suleimenov and Krupp[11]. In this work, we conduct the same volume calculation by using PR EOS coupled with the HV mixing rule (Case 3) with/without volume

translation. In addition to the constant volume translation model, we also investigate the predictive ability of the volume translation model proposed by Abudour *et al.*[20]

Table 6 compares the calculated phase composition and total volumes from Zhao *et al.*[2] model (denoted as $V_{cal,Zhao}$), Case 3 without volume translation (denoted $V_{cal,UT}$), Case 3 with constant volume translation model (denoted as $V_{cal,VT1}$) and Case 3 with Abudour *et al.* volume translation model[20] (denoted as $V_{cal,VT2}$), together with the experimental data (denoted as $y_{1,exp}$, $x_{2,exp}$ and V_{exp}) measured by Suleimenov and Krupp[11]. As mentioned earlier, Zhao *et al.*[2] model shows a relatively large error in reproducing the measured total volume data. From the results shown in **Table 6**, we can see that Case 3 without volume translation improves the accuracy of the total volume calculation by reducing the *%AAD* from 13.64% given by Zhao *et al.*[2] model to 8.36%. Case 3 with the constant volume translation model yields a much lower %*AAD* of 4.05% compared to 13.64% given by Zhao *et al.*[2] model. The implementation of Abudour *et al*. volume translation model[20] in Case 3 yields the lowest *%AAD* of 2.01%. **Figure 9** presents the corresponding *%AADs* in reproducing the total volumes of the H_2S/H_2O mixture by different modelling strategies, which again shows that the highest accuracy in reproducing the measured total volumes[11] can be achieved by PR EOS coupled with the Twu alpha function[21], the optimized HV mixing rule[22], and the Abudour *et al*. volume translation model[20].

Table 6. Comparisons of measured phase compositions and total volumes of H_2S/H_2O mixtures[11] against calculated ones from different modelling strategies.

T (K)	P (bar)	nH_2S (mol)	nH_2O (mol)	$y_{1,exp}$[a] *100	$y_{1,cal}$[b] *100	$x_{2,exp}$[a] *100	$x_{2,cal}$[b] *100	V_{exp}[a] (cm^3)	$V_{cal,Zhao}$[c] (cm^3)	$V_{cal,UT}$[b] (cm^3)	$V_{cal,VT1}$[d] (cm^3)	$V_{cal,VT2}$[e] (cm^3)
293.95	4.25	0.0163	1.248	0.610	0.621	0.898	0.862	50.8	59.7	57.3	46.3	54.7
294.45	4.29	0.0157	1.1716	0.630	0.635	0.852	0.859	52.7	57.8	56.0	50.9	52.8
294.55	2.6	0.0093	1.058	1.020	1.029	0.509	0.510	55.5	59.9	58.8	54.3	55.9
295.45	4.96	0.001749	1.05	0.580	0.589	0.989	0.972	52.8	57.8	49.1	54.3	51.4
295.55	3.93	0.0173	1.6657	0.690	0.737	0.765	0.761	57.7	64.3	63.4	56.5	58.9
295.95	5.41	0.0185	1.0167	0.550	0.560	1.030	1.051	53.4	56.1	55.6	54.7	55.5
295.95	7.9	0.0299	1.1007	0.390	0.398	1.555	1.568	57.1	61.2	60.0	58.1	57.1
296.65	2.95	0.0125	1.6602	0.970	1.034	0.548	0.550	57.9	62.1	63.0	60.7	58.5
297.35	2.22	0.00808	1.1206	1.400	1.419	0.413	0.403	58.5	62	63.4	57.9	60.3
308.75	5.56	0.0179	1.663	1.120	1.133	0.766	0.786	53.3	58.5	57.2	56.6	52.7
313.15	4.53	0.01313	1.2329	1.720	1.737	0.607	0.576	54.4	60	60.6	60.0	53.5
333.35	5	0.0125	1.6602	4.200	4.260	0.459	0.424	57.9	64.1	66.9	66.7	58.0
357.75	9.48	0.01313	1.2329	6.390	6.514	0.653	0.618	54.4	43.5	45.1	62.3	55.7
358.95	8.66	0.01749	1.05	7.290	7.414	0.584	0.554	52.8	63.6	61.6	58.9	53.3
373.95	7.44	0.0125	1.6602	14.590	14.767	0.415	0.397	57.9	64.5	65.5	51.9	57.4

413.95	15.91	0.0179	1.663	24.650	24.983	0.615	0.628	53.3	59	59.5	56.6	52.2
415.75	15.82	0.0179	1.663	26.010	26.361	0.629	0.610	53.3	60.5	61.0	57.9	53.7
423.95	16.06	0.0173	1.6657	31.830	32.237	0.547	0.558	57.7	63	64.1	62.4	58.6
424.15	16.03	0.0173	1.6657	32.050	32.458	0.550	0.555	57.7	63.3	64.4	62.7	58.9
426.75	13.3	0.0125	1.6602	40.680	41.176	0.399	0.399	57.9	64	64.9	51.7	57.3
428.25	16.36	0.01749	1.05	34.900	35.339	0.529	0.538	52.8	62.1	59.6	58.2	52.5
425.88	11.59	0.0093	1.058	48.350	45.790	0.303	0.321	55.5	59.9	56.9	56.9	54.6
429.35	18.04	0.0179	1.663	32.800	33.235	0.635	0.611	53.3	60.8	58.4	54.3	54.2
440.25	20.45	0.0179	1.663	38.070	38.570	0.632	0.626	53.3	60.9	57.8	54.0	53.6
466.65	27.28	0.0185	1.0167	52.130	52.795	0.641	0.634	53.4	58.9	58.6	54.4	54.6
469.35	27.99	0.01313	1.2329	53.790	54.459	0.618	0.628	54.4	46.8	61.6	59.0	55.8
471.35	28.45	0.01749	1.05	55.150	55.831	0.603	0.620	52.8	58.1	57.7	51.3	51.7
472.95	21.12	0.00808	1.1206	74.240	75.104	0.248	0.260	58.5	46.6	63.9	58.5	60.2
479.35	27.07	0.0125	1.6602	67.140	67.930	0.412	0.431	57.9	66	64.9	59.5	57.2
489.65	27.55	0.00808	1.1206	79.730	80.584	0.248	0.269	58.5	65	63.8	58.5	60.0
494.25	37.42	0.01749	1.05	66.140	66.903	0.651	0.627	52.8	60.3	55.2	52.9	53.4
502.75	42.59	0.0185	1.0167	68.410	69.094	0.669	0.679	53.4	59.9	51.0	52.7	52.2
505.55	43.24	0.0163	1.248	70.680	71.367	0.664	0.642	50.8	58.9	47.3	51.4	51.8

507.45	44.98	0.0179	1.663	70.510	71.176	0.770	0.676	53.3	64.9	51.5	53.7	51.3
507.85	44.81	0.01749	1.05	71.210	71.851	0.649	0.658	52.8	59.6	54.6	52.4	52.7
515.65	49.29	0.01749	1.05	74.220	74.885	0.682	0.660	52.8	60.3	55.5	53.3	53.6
515.75	49.46	0.01749	1.05	74.130	74.787	0.675	0.665	52.8	59.9	55.2	53.0	53.3
527.95	56.89	0.01749	1.05	79.070	79.674	0.663	0.643	52.8	63	58.7	56.1	49.8
529.55	55.11	0.01313	1.2329	82.920	83.552	0.513	0.507	54.4	62.1	50.0	53.9	56.8
537.25	72.58	0.0299	1.1007	74.000	74.784	1.185	1.064	57.1	66.1	53.3	55.8	56.1
539.15	62.63	0.01313	1.2393	85.270	85.834	0.532	0.517	54.4	62.9	50.9	54.8	52.4
546.15	73.33	0.01749	1.05	82.680	83.094	0.710	0.750	52.8	58.4	54.6	52.5	52.4
547.75	65.41	0.00724	1.1426	92.080	92.470	0.287	0.298	54.6	61.7	51.1	54.7	55.8
552.25	86.35	0.0299	1.1007	78.840	79.330	1.259	1.123	57.1	67.1	53.6	56.3	58.8
564.95	89.38	0.0157	1.1716	89.020	89.385	0.775	0.641	52.7	66	53.0	52.5	53.8
573.85	99.92	0.0157	1.1716	90.510	90.789	0.802	0.665	52.7	66.4	49.5	52.6	54.1
584.05	112.86	0.0157	1.1716	92.230	92.443	0.856	0.673	52.7	68.9	55.4	51.2	51.2
594.15	138.61	0.0299	1.1007	88.960	89.098	1.536	1.351	57.1	69.4	55.8	57.8	55.8
%AAD					**1.40%**		**4.55%**		**13.64%**	**8.36%**	**4.05%**	**2.01%**

a: The experimental phase equilibria and total volume data were reported by Suleimenov and Krupp[11].
b: Phase compositions and total volume results calculated from PR EOS and the HV mixing rule (Case 3).
c: Total volumes calculated by Zhao *et al*.[2]
d: Total volumes calculated by PR EOS, the HV mixing rule (Case 3), and the constant volume translation model.
e: Total volumes calculated by PR EOS, the HV mixing rule (Case 3), and the Abudour *et al.* volume translation model[20].

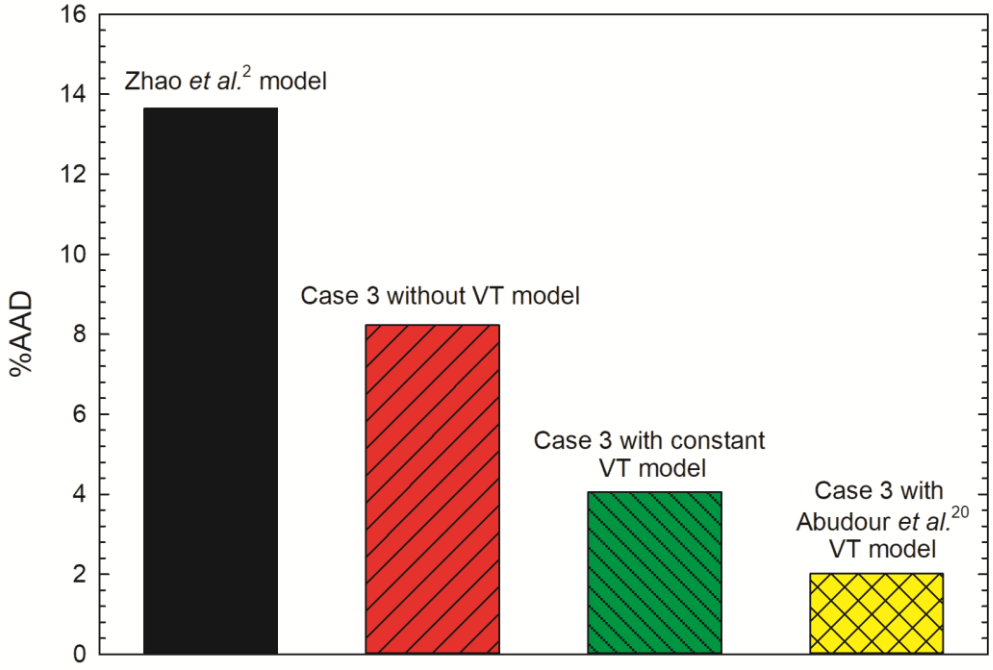

Figure 9. Comparison of *%AADs* in reproducing the measured total volumes of a H_2S/H_2O mixture[11] by different modelling strategies.

Table 7 lists the calculated aqueous-phase density data from Case 3 with the constant volume translation model (denoted as $\rho_{aq,VT1}$) and Case 3 with the Abudour *et al.* volume translation model[20] (denoted as $\rho_{aq,VT2}$), together with the experimental data (denoted as $\rho_{aq,exp}$) reported in the literature[16-18]. As mentioned earlier, we only calculate the aqueous phase density of the H_2S/H_2O mixtures below 600 K. The results in **Table 7** show that Case 3 with the constant volume translation model yields an *%AAD* of 13.67% in reproducing the measured aqueous phase density data for the H_2S/H_2O system. Case 3 coupled with the Abudour *et al.* volume translation model[20] generally provides a good agreement with the measured aqueous phase density data over a wide range of temperature and pressure; an *%AAD* of 5.42% can be obtained. However, at elevated temperatures and pressures (above 473.15 K and 200 bar), the calculated

aqueous phase densities from Abudour *et al.*[20] volume translation model show relatively larger errors than those at lower temperatures. A similar issue also exists for the constant volume translation model at temperatures above 523.15 K and pressures above 200 bar. In summary, the above results clearly demonstrate that the PR EOS coupled with the Twu alpha function[21], the optimized HV mixing rule[22], and the Abudour *et al*. volume translation model[20] is a reliable and consistent thermodynamic tool for simulating the VLE/LLE and density of H_2S/H_2O mixtures over a wide range of temperatures and pressures.

Table 7. Performance comparisons of different modeling strategies in predicting the measured density data for H_2S/H_2O mixtures[16-18].

T (K)	P (bar)	$\rho_{aq,exp}$ (g/cm^3)[a]	$\rho_{aq,VT1}$ (g/cm^3)[b]	$\rho_{aq,VT2}$ (g/cm^3)[c]	References
294.35	4.46	0.998	1.134	0.978	[17]
294.45	1.01	0.998	1.130	0.975	[17]
294.45	7.90	0.998	1.137	0.981	[17]
298.15	10.00	0.997	1.134	0.980	[18]
298.15	200.00	1.006	1.147	0.991	[18]
298.15	350.00	1.012	1.151	0.994	[18]
298.85	7.90	0.997	1.132	0.978	[17]
298.85	11.35	0.997	1.135	0.980	[17]
298.95	4.46	0.997	1.129	0.975	[17]
298.95	14.79	0.997	1.137	0.983	[17]
299.25	1.01	0.997	1.126	0.972	[17]
300.65	7.90	0.996	1.130	0.976	[17]
300.65	11.35	0.996	1.133	0.979	[17]
300.65	14.79	0.996	1.135	0.981	[17]
300.75	18.24	0.996	1.137	0.984	[17]
300.85	4.46	0.996	1.127	0.973	[17]
301.05	1.01	0.996	1.124	0.970	[17]
305.25	18.24	0.995	1.132	0.979	[17]
305.35	14.79	0.995	1.129	0.977	[17]
305.55	11.35	0.995	1.127	0.975	[17]
305.85	7.90	0.995	1.124	0.972	[17]
306.15	4.46	0.994	1.121	0.969	[17]
306.65	1.01	0.994	1.118	0.966	[17]
310.95	18.80	0.994	1.125	0.974	[16]
312.45	18.24	0.992	1.123	0.973	[17]
312.65	14.79	0.992	1.120	0.971	[17]
312.95	11.35	0.992	1.118	0.968	[17]
313.35	7.90	0.992	1.116	0.966	[17]
313.75	4.46	0.992	1.113	0.964	[17]
314.15	1.01	0.992	1.110	0.961	[17]

323.15	200.10	0.996	1.122	0.974	[18]
323.15	350.00	1.002	1.127	0.978	[18]
373.15	200.00	0.967	1.062	0.9344	[18]
373.15	350.00	0.973	1.069	0.940	[18]
377.55	40.70	0.941	1.045	0.919	[16]
377.55	81.20	0.939	1.049	0.925	[16]
377.55	103.40	0.929	1.050	0.926	[16]
410.95	49.60	0.909	0.997	0.885	[16]
410.95	97.80	0.901	0.998	0.889	[16]
410.95	123.80	0.896	0.998	0.891	[16]
423.15	200.00	0.926	0.978	0.878	[18]
423.15	350.00	0.934	0.988	0.886	[18]
444.25	58.00	0.859	0.942	0.847	[16]
444.25	103.40	0.857	0.938	0.847	[16]
444.25	130.00	0.857	0.935	0.847	[16]
473.15	199.90	0.926	0.857	0.795	[18]
473.35	349.90	0.886	0.847	0.790	[18]
523.15	199.90	0.813	0.688	0.671	[18]
523.15	350.00	0.827	0.700	0.659	[18]
532.05	280.10	0.810	0.660	0.647	[18]
573.15	200.00	0.731	0.559	0.566	[18]
573.15	349.90	0.754	0.429	0.439	[18]
578.88	280.00	0.732	0.393	0.410	[18]
%AAD			**13.67%**	**5.42%**	

a: The experimental aqueous phase density data taken from Clark[16], Murphy and Gaines[17], and Wood and Majer[18].
b: The calculated aqueous phase density results from Case 3 with constant volume translation model.
c: The calculated aqueous phase density results from Case 3 with Abudour *et al*. volume translation model[20].

References

[1] Selleck, F. T.; Carmichael, L. T.; Sage, B. H. Phase Behavior in the Hydrogen Sulfide-Water System. *Ind*. *Eng. Chem*. **1952**, *44*, 2219-2226.

[2] Zhao, H.; Fang, Z.; Jing, H.; Liu, J. Modeling Vapor-Liquid Phase Equilibria of Hydrogen Sulfide and Water System Using a Cubic EOS-G^{EX} Model. *Fluid Phase Equilib.* **2019**, *484*, 60-73.

[3] Wright, R. H.; Maass, O. The Solubility of Hydrogen Sulphide in Water from the Vapor Pressures of the Solutions. *Can. J. Res*. **1932**, *6*, 94-101.

[4] Burgess, M. P.; Germann, R. P. Physical Properties of Hydrogen Sulfide-Water Mixtures. *AIChE J.* **1969**, *2*, 272-275.

[5] Clarke, E. C. W.; Glew, D. N. Aqueous Nonelectrolyte Solutions. Part VIII. Deuterium and Hydrogen Sulfides Solubilities in Deuterium Oxide and Water. *Can. J. Chem*. **1971**, *49*, 691-698.

[6] Lee, J. L.; Mather, A. E. Solubility of Hydrogen Sulfide in Water. *Ber. Bunsenges. Phys. Chem*. **1977**, *81*, 1020-1023.

[7] Drummond, S. E. Boiling and Mixing of Hydrothermal Fluids: Chemical Effects on Mineral Precipitation. *Ph. D. Dissertation. Geoscience. Pennsylvania State University* **1981**.

[8] Gillespie, P. C.; Owens, J. L.; Wilson, G. M. Sour Water Equilibria Extended to High Temperatures and with Inerts Present. *AIChE Winter Mtg*., *Atlanta, GA*. **1984**.

[9] Barrett, T. J.; Anderson, G.; Lugowski, M. J. The Solubility of Hydrogen Sulphide in 0–5 m NaCl Solutions at 25–95 °C and One Atmosphere. *Geoch. Cosm. Acta*. **1988**, *52*, 807-811.

[10] Carroll, J. J.; Mather, A. E. Phase Equilibrium in the System Water-Hydrogen Sulphide: Modelling the Phase Behavior with an Equation of State. *Can. J. Chem. Eng.* **1989**, *57*, 999-1003.

[11] Suleimenov, O. M.; Krupp, R. E. Solubility of Hydrogen Sulfide in Pure Water and in NaCl Solutions, from 20 to 320 ºC and at Saturation Pressures. *Geoch. Cosm. Acta*. **1994**, *58*, 2433-2444.

[12] Kuranov, G.; Rumpf, B.; Smirnova, N. A.; Maurer, G. Solubility of Single Gases Carbon Dioxide and Hydrogen Sulfide in Aqueous Solutions of N-methyldiethanolamine in the

Temperature Range 313−413 K at Pressures up to 5 MPa. *Ind. Eng. Chem. Res*. **1996**, *35*, 1959-1966.

[13] Chapoy, A.; Mohammadi, A. H.; Tohidi, B.; Valtz, A.; Richon, D. Experimental Measurement and Phase Behavior Modeling of Hydrogen Sulfide−Water Binary System. *Ind. Eng. Chem. Res.* **2005**, *44*, 7567-7574.

[14] Koschel, D.; Coxam, J. Y.; Majer, V. Enthalpy and Solubility Data of H_2S in Water at Conditions of Interest for Geological Sequestration. *Ind. Eng. Chem. Res*. **2007**, *46*, 1421-1430.

[15] Savary, V.; Berger, G.; Dubois, M.; Lacharpagne, J. C.; Pages, A.; Thibeau, S.; Lescanne, M. The Solubility of CO_2+H_2S Mixtures in Water and 2 M NaCl at 120°C and Pressures up to 35 MPa. *Int. J. Greenh. Gas Cont*. **2012**, *10*, 123-133.

[16] Clark, S. P. Handbook of Physical Constants. *Geol. Soc*. **1966**.

[17] Murphy, J. A.; Gaines Jr, G. L. Density and Viscosity of Aqueous Hydrogen Sulfide Solutions at Pressures to 20 atm. *J. Chem. Eng. Data* **1974**, *19*, 359-362.

[18] Wood, R. H.; Majer, V. Volumes of Aqueous Solutions of CH_4, CO_2, H_2S and NH_3 at Temperatures from 298.15 K to 705 K and Pressures to 35 MPa. *J. Chem. Thermodyn*. **1996**, *28*, 125-142.

[19] Wong, D. S. H.; Sandler, S. I. A Theoretically Correct Mixing Rule for Cubic Equation of State. *AIChE J*. **1992**, *5*, 671-680.

[20] Abudour, A. M.; Mohammad, S. A.; Robinson Jr, R. L.; Khaled, A. M. G. Volume-Translated Peng-Robinson Equation of State for Liquid Densities of Diverse Binary Mixtures. *Fluid Phase Equilib*. **2013**, *349*, 37-55.

[21] Twu, C. H.; Bluck, D.; Cunningham, J. R.; Coon, J. E. A Cubic Equation of State with a New Alpha Function and a New Mixing Rule. *Fluid Phase Equilib*. **1991**, *69*, 33-50.

[22] Huron, M. J.; Vidal, J. New Mixing Rules in Simple Equations of State for Representing Vapour-Liquid Equilibria of Strongly Non-Ideal Mixtures. *Fluid Phase Equilib*. **1979**, *3*, 255-271.

CHAPTER 4 CONCLUSIONS AND RECOMMENDATIONS

4.1 Conclusions

Different modeling strategies are tried in this study to determine the optimal thermodynamic model that can well capture the phase behaviour of H_2S/H_2O mixtures. Based on the results obtained in this study, we can reach the following conclusions:

1) Different BIP (c and k_{ij}) strategies in the HV mixing rule are tried in PR EOS to model the VLE/LLE of H_2S/H_2O mixtures. The linear temperature dependence of k_{ij} coupled with a constant c in the HV mixing rule (corresponding to Case 3 BIP strategy in this study) is recommended as the most accurate BIP strategy since it leads to the best reproduction of the measured VLE/LLE data for H_2S/H_2O mixtures.
2) By comparing the calculated results against the experimental data for H_2S/H_2O mixtures reported in the literature, we find that the optimal model (i.e., PR EOS+Twu alpha function+HV mixing rule+Case 3 BIP) is able to decently reproduce the measured phase behavior data of H_2S/H_2O system at temperatures up to 627.85 K and pressures up to 302.7 bar. This model yields an *%AAD* of 4.90% and an %*AAD* of 4.95% in reproducing H_2S solubility in the aqueous phase and H_2O solubility in the H_2S-rich phase, respectively.
3) Case 3 BIP strategy also shows good performance in reproducing the measured volume data for several H_2S/H_2O mixtures[1]. Even without any volume translation model, Case 3 BIP strategy reduces the *%AAD* from 13.64% given by Zhao *et al*. model[2] to 8.36%. Coupled with the constant volume translation model, Case 3 provides an *%AAD* of 4.05% in estimating the volumes of H_2S/H_2O mixtures. The employment of Abudour *et al.*

volume translation model[3] with Case 3 BIP strategy further reduces the %*AAD* yielded by Zhao *et al.* model[2] by more than 85% (i.e., from 13.64% to 2.01%).

4) As for the aqueous-phase density calculations, the combination of Case 3 BIP strategy with different volume translation models allows for fairly accurate prediction of the aqueous-phase density of H_2S/H_2O mixtures. More specifically, yielding an *%AAD* of 5.42% in reproducing the measured density data, Case 3 with the Abuduour *et al.*[3] volume translation model provides the best performance in estimating aqueous-phase density. However, at 473.15+ K and 200+ bar, Abuduour *et al.*[3] volume translation model tends to underestimate the aqueous-phase density, making its prediction less reliable under these conditions. Overall, Case 3 BIP strategy together with the volume translation model proposed by Abudour *et al.*[3] is capable of providing a good accuracy in calculating aqueous-phase density of H_2S/H_2O mixtures up to 473.15 K and 200 bar.
5) By simply refitting the parameters (i.e., c and k_{ij}) in HV mixing rule to the experimental phase behavior data measured for other gas/water binaries mixtures (e.g., CO_2/H_2O mixtures), the thermodynamic modeling framework used in this thesis can be potentially applied to well reproduce the VLE/LLE of these binary mixtures.

4.2 Recommendations

More experimental phase equilibrium data of H_2S/H_2O mixtures are needed to examine the performance of Case 3 BIP strategy, especially at 100+ bar. Furthermore, Case 3 is potentially valid for reproducing the measured VLE/LLE data of H_2S/brine mixtures over a wide range of temperatures and pressures. Hence, the effect of salinity on phase equilibria of H_2S/H_2O mixtures could be considered in the future modeling work.

As for aqueous-phase density estimation, more experimental data are needed to examine the ability of Case 3 with Abudour *et al*.[3] volume translation model in density prediction. In addition, some further modifications to Abudour *et al*.[3] volume translation model are desired such that the volume translation-PR EOS can become capable of more accurately predicting the aqueous-phase density of H_2S/H_2O mixtures at high temperatures (473.15+ K) and pressures (200+ bar).

References

[1] Suleimenov, O. M.; Krupp, R. E. Solubility of Hydrogen Sulfide in Pure Water and in NaCl Solutions, from 20 to 320 ºC and at Saturation Pressures. *Geoch. Cosm. Acta*. **1994**, *58*, 2433-2444.

[2] Zhao, H.; Fang, Z.; Jing, H.; Liu, J. Modeling Vapor-Liquid Phase Equilibria of Hydrogen Sulfide and Water System Using a Cubic EOS-G^{EX} Model. *Fluid Phase Equilib.* **2019**, *484*, 60-73.

[3] Abudour, A. M.; Mohammad, S. A.; Robinson Jr, R. L.; Khaled, A. M. G. Volume-Translated Peng-Robinson Equation of State for Liquid Densities of Diverse Binary Mixtures. *Fluid Phase Equilib*. **2013**, *349*, 37-55.

BIBLIOGRAPHY

Abudour, A. M.; Mohammad, S. A.; Robinson Jr, R. L.; Khaled, A. M. G. Volume-Translated Peng-Robinson Equation of State for Saturated and Single-Phase Liquid Densities. *Fluid Phase Equilib*. **2012**, *335*, 74-87.

Abudour, A. M.; Mohammad, S. A.; Robinson Jr, R. L.; Khaled, A. M. G. Volume-Translated Peng-Robinson Equation of State for Liquid Densities of Diverse Binary Mixtures. *Fluid Phase Equilib*. **2013**, *349*, 37-55.

Abudour, A. M.; Sayee, A. M.; Khaled, A. M. G. Modeling High-Pressure Phase Equilibria of Coalbed Gases/Water Mixtures with the Peng–Robinson Equation of State. *Fluid Phase Equilib.* **2012**, *319*, 77-89.

Akinfiev, N. N.; Majer, V.; Shvarov, Y. V. Thermodynamic Description of H_2S–H_2O–NaCl Solutions at Temperatures to 573 K and Pressures to 40 MPa. *Chem. Geol.* **2016**, *424*, 1-11.

Baled, H.; Enick, R. M.; Wu, Y.; McHugh, M. A.; Burgess, W.; Tapriyal, D.; Morreale, B. D. Prediction of Hydrocarbon Densities at Extreme Conditions Using Volume-Translated SRK and PR Equation of State Fit to High Temperature, High Pressure PVT Data. *Fluid Phase Equilib*. **2012**, *317*, 65-76.

Barrett, T. J.; Anderson, G.; Lugowski, M. J. The Solubility of Hydrogen Sulphide in 0–5 m NaCl Solutions at 25–95 C and One Atmosphere. *Geoch. Cosm. Acta*. **1988**, *52*, 807-811.

Beauchamp, R. O.; James, S. B.; James, A. P.; Craig A. J. B.; Dragana, A. A.; Philip, L. A Critical Review of the Literature on Hydrogen Sulfide Toxicity. *Crit. Rev. Toxicol.* **1984**, *13*, 25-97.

Burgess, M. P.; Germann, R. P. Physical Properties of Hydrogen Sulfide-Water Mixtures. *AIChE J*. **1969**, *2*, 272-275.

Carroll, J. J.; Mather, A. E. Phase Equilibrium in the System Water-Hydrogen Sulphide: Modelling the Phase Behavior with an Equation of State. *Can. J. Chem. Eng.* **1989**, *57*, 999-1003.

Chapoy, A.; Mohammadi, A. H.; Tohidi, B.; Valtz, A.; Richon, D. Experimental Measurement and Phase Behavior Modeling of Hydrogen Sulfide−Water Binary System. *Ind. Eng. Chem. Res.* **2005**, *44*, 7567-7574.

Chou, G. F.; Prausnitz, J. M. A Phenomenological Correction to an Equation of State for the Critical Region. *AIChE J*. **1989**, *35*, 1487-1496.

Clark, S. P. Handbook of Physical Constants. *Geol. Soc*. **1966**.

Clarke, E. C. W.; Glew, D. N. Aqueous Nonelectrolyte Solutions. Part VIII. Deuterium and Hydrogen Sulfides Solubilities in Deuterium Oxide and Water. *Can. J. Chem*. **1971**, *49*, 691-698.

Drummond, S. E. Boiling and Mixing of Hydrothermal Fluids: Chemical Effects on Mineral Precipitation. *Ph. D. Dissertation. Geoscience. Pennsylvania State University* **1981**.

Duan, Z.; Hu, J.; Li, D.; Mao, S. Densities of the CO_2–H_2O and CO_2–H_2O–NaCl Systems up to 647 K and 100 MPa. *Energy Fuels* **2008**, *22*, 1666-1674.

Duan, Z.; Sun, R.; Liu, R.; Zhu, C. Accurate Thermodynamic Model for the Calculation of H_2S Solubility in Pure Water and Brines. *Energy Fuels* **2007**, *21*, 2056-2065.

Ewing, S. P. Electrochemical Studies of the Hydrogen Sulfide Corrosion Mechanism. *Corrosion* **1955**, *11*, 51-55.

Fu, W.; Wang, Z.; Zhang, J.; Cao, Y.; Sun, B. Investigation of Rheological Properties of Methane Hydrate Slurry with Carboxmethylcellulose. *J. Pet. Sci. Eng.* **2020**, *184*, 106504.

Gillespie, P. C.; Owens, J. L.; Wilson, G. M. Sour Water Equilibria Extended to High Temperatures and with Inerts Present. *AIChE Winter Mtg*., *Atlanta, GA*. **1984**.

Huron, M. J.; Vidal, J. New Mixing Rules in Simple Equations of State for Representing Vapour-Liquid Equilibria of Strongly Non-Ideal Mixtures. *Fluid Phase Equilib*. **1979**, *3*, 255-271.

Koschel, D.; Coxam, J. Y.; Majer, V. Enthalpy and Solubility Data of H_2S in Water at Conditions of Interest for Geological Sequestration. *Ind. Eng. Chem. Res*. **2007**, *46*, 1421-1430.

Kuranov, G.; Rumpf, B.; Smirnova, N. A.; Maurer, G. Solubility of Single Gases Carbon Dioxide and Hydrogen Sulfide in Aqueous Solutions of N-methyldiethanolamine in the Temperature Range 313−413 K at Pressures up to 5 MPa. *Ind. Eng. Chem. Res*. **1996**, *35*, 1959-1966.

Lee, J. L.; Mather, A. E. Solubility of Hydrogen Sulfide in Water. *Ber. Bunsenges. Phys. Chem*. **1977**, *81*, 1020-1023.

Li, R.; Li, H. Improved Three-Phase Equilibrium Calculation Algorithm for Water/Hydrocarbon Mixtures. *Fuel* **2019**, *15*, 517-527.

Lin, H.; Duan, Y. Y. Empirical Correction to the Peng-Robinson Equation of State for the Saturated Region. *Fluid Phase Equilib*. **2005**, *233*, 194-203.

Lindeloff, N.; Michelsen, M. L. Phase Envelope Calculations for Hydrocarbon-Water Mixtures. *SPE J*. **2003**, *8*, 298-303.

Magoulas, K.; Tassios, D. Thermophysical Properties of Normal-Alkanes from C_1 to C_{20} and Their Prediction for Higher Ones. *Fluid Phase Equilib*. **1990**, *56*, 119-140.

Martinez, A. P.; Guennec, Y. L.; Privat, R.; Jaubert, J. N.; Mathias, P. M. Analysis of the Combinations of Property Data that Are Suitable for a Safe Estimation of Consistent Twu α-Function Parameters: Updated Parameter Values for the Translated-Consistent tc-PR and tc-RK Cubic Equations of State. *J. Chem. Eng. Data* **2018**, *63*, 3980-3988.

Murphy, J. A.; Gaines Jr, G. L. Density and Viscosity of Aqueous Hydrogen Sulfide Solutions at Pressures to 20 atm. *J. Chem. Eng. Data* **1974**, *19*, 359-362.

Ning, J.; Zheng, Y.; Young, D.; Brown, B.; Nešić, S. Thermodynamic Study of Hydrogen Sulfide Corrosion of Mild Steel. *Corrosion* **2013**, *70*, 375-389.

Peneloux, A.; Rauzy, E.; Freze, R. A Consistent Correction for Redlich-Kwong-Soave Volume. *Fluid Phase Equilib*. **1982**, *8*, 7-23.

Peng, D. Y.; Robinson, D. B. A New Two-Constant Equation of State. *Ind. Eng. Chem. Fundam.* **1976**, *15*, 59–64.

Rachford Jr, H. H.; Rice, J. D. Procedure for Use of Electronic Digital Computers in Calculating Flash Vaporization Hydrocarbon Equilibrium. *J. PET. Technol*. **1952**, *410*, 19-3.

Reiffenstein, R. J.; William, C.H.; Sheldon, H. R. Toxicology of Hydrogen Sulfide. *Annu. Rev Pharmacol.* **1992**, *32*, 109-134.

Savary, V.; Berger, G.; Dubois, M.; Lacharpagne, J. C.; Pages, A.; Thibeau, S.; Lescanne, M. The Solubility of CO_2+H_2S Mixtures in Water and 2 M NaCl at 120° C and Pressures up to 35 MPa. *Int. J. Greenh. Gas Cont*. **2012**, *10*, 123-133.

Selleck, F. T.; Carmichael, L. T.; Sage, B. H. Phase Behavior in the Hydrogen Sulfide-Water System. *Ind. Eng. Chem*. **1952**, *44*, 2219-2226.

Shi, J.; Li, H.; Pang, W. An Improved Translation Strategy for PR EOS without Crossover Issue. *Fluid Phase Equilib*. **2018**, *470*, 164-175.

Soave, G. Equilibrium Constants from a Modified Redlich-Kwong Equation of State. *Chem. Eng. Sci.***1972**, *27*, 1197-1203.

Søreide, I.; Whitson, C. H. Peng-Robinson Predictions for Hydrocarbons, CO_2, N_2, and H_2S with Pure Water and NaCl Brine. *Fluid Phase Equilib.* **1992**, *77*, 217-240.

Suleimenov, O. M.; Krupp, R. E. Solubility of Hydrogen Sulfide in Pure Water and in NaCl Solutions, from 20 to 320 ºC and at Saturation Pressures. *Geoch. Cosm. Acta*. **1994**, *58*, 2433-2444.

Tsai, J. C.; Chen, Y. P. Application of a Volume-Translated Peng-Robinson Equation of State on Vapor-Liquid Equilibrium Calculations. *Fluid Phase Equilib*. **1998**, *145*, 193-215.

Twu, C. H.; Bluck, D.; Cunningham, J. R.; Coon, J. E. A Cubic Equation of State with a New Alpha Function and a New Mixing Rule. *Fluid Phase Equilib*. **1991**, *69*, 33-50.

Wang, Z.; Zhang, J.; Sun, B.; Chen, L.; Zhao, Y., Fu, W. A New Hydrate Deposition Prediction Model for Gas-Dominated Systems with Free Water. *Chem. Eng. Sci.* **2017**, *163*, 145-154.

Whitson, C. H.; Brulé, M. R. Phase Behavior (Vol. 20). Richardson, TX: Henry L. Doherty Memorial Fund of AIME. *SPE*. **2000**.

Wilson, G. M. A Modified Redlich-Kwong Equation of State, Application to General Physical Data Calculations. *65th National AIChE Meeting, Cleveland,* **1969***,15*.

Wong, D. S. H.; Sandler, S. I. A Theoretically Correct Mixing Rule for Cubic Equation of State. *AIChE J*. **1992**, *5*, 671-680.

Wood, R. H.; Majer, V. Volumes of Aqueous Solutions of CH_4, CO_2, H_2S and NH_3 at Temperatures from 298.15 K to 705 K and Pressures to 35 MPa. *J. Chem. Thermodyn*. **1996**, *28*, 125-142.

Wright, R. H.; Maass, O. The Solubility of Hydrogen Sulphide in Water from the Vapor Pressures of the Solutions. *Can. J. Res*. **1932**, *6*, 94-101.

Young, A. F.; Pessoa, F. L. P.; Ahón, V .R. R. Comparison of Volume Translation and Co-Volume Functions Applied in the Peng-Robinson EOS for Volumetric Corrections. *Fluid Phase Equilib*. **2017**, *435*, 73-87.

Zhang, J.; Wang, Z.; Liu, S.; Zhang, W.; Yu, J.; Sun, B. Prediction of Hydrate Deposition in Pipelines to Improve Gas Transportation Efficiency and Safety. *Appl. Energy* **2019**, *253,* 113521.

Zhao, H.; Fang, Z.; Jing, H.; Liu, J. Modeling Vapor-Liquid Phase Equilibria of Hydrogen Sulfide and Water System Using a Cubic EOS-G^{EX} Model. *Fluid Phase Equilib.* **2019**, *484*, 60-73.